

Exocyst dysfunction impairs urothelial development resulting in congenital ureter obstruction

A MASTER'S THESIS SUBMITTED TO THE GRADUATE DIVISION OF THE UNIVERSITY OF HAWAI'I
AT MĀNOA IN PARTIAL FULFILLMENT OF THE REQUIREMENTS FOR THE DEGREE OF

MASTERS OF SCIENCE

IN

DEVELOPMENTAL AND REPRODUCTIVE BIOLOGY

AUGUST 2016

By

Josephine Andrea Napoli

Thesis Committee

Ben Fogelgren, Chairperson

Scott Lozanoff

Yusuke Marikawa

Acknowledgments

This Master's Thesis is dedicated to each of the people who have loved, supported, taught and inspired me. I would like to express my deep appreciation and gratitude to the people who guided me to this point and to whom I owe all my past and future success.

My family

To my parents, who fostered my sense of curiosity and who have supported me in every one of my endeavors. Thank you for a lifetime of unconditional love and encouragement, and for showing me that I could do anything.

To my siblings, who make being a super-nerd cool. By including me in your amazing accomplishments, you taught me a lesson that would not have had the same impact from anyone else: when families build each other up, all our achievements are that much more satisfying. Thank you for your example and for teaching me to think (and dream) bigger.

And, to my fiancé, who can always be found in the front row. Thank you for coming on this adventure with me, and for all the sacrifices you have made to help me succeed.

My mentors

To my committee members, Dr. Yusuke Marikawa and Dr. Scott Lozanoff for believing in me. I am so incredibly grateful that you gave me a chance by accepting me into this program, offering me a teaching position, and investing so much time in me. Thank you for asking me the hard questions and for your ongoing support.

To the entire Fogelren Lab, who stood by my side every day for these past two years, training and advising me, and made my success a priority. For that, I am so grateful.

To my advisor, Dr. Ben Fogelgren, who has given unparalleled guidance and mentorship. I am truly fortunate to have had the opportunity to work with a mentor of his caliber, not just as a scientist but as a human being. Thank you for challenging me, inspiring me, and for being my role model.

Abstract

Hydronephrosis is the most commonly detected abnormality in prenatal ultrasounds. The most prevalent cause of prenatal hydronephrosis is congenital obstructive nephropathy, with obstructions at the ureteropelvic junction (UPJ) region as the most common site for obstruction. The cause and developmental process of obstruction formation at the UPJ is poorly understood.

We developed a Sec10 conditional knockout (Sec10-CKO) mouse model where Sec10, a critical subunit of the exocyst complex, has been knocked out in the urothelium that lines the ureter. Sec10-CKO embryos develop complete bilateral UPJ obstructions and hydronephrosis by day 18.5 of gestation (E18.5).

Using this model, we were able to study the development of prenatal hydronephrosis. We determined that the urothelium lining the ureters of Sec10-CKO mice fails to differentiate, with the earliest evidence of this starting at E16.5. Loss of key terminal differentiation markers, including uroplakins, weakens the urothelial barrier that prevents urine from permeating into ureter tissues. Our data suggests that a luminal wound healing response at the UPJ starts at E17.5, which would correspond with the time point urine first starts to flow. We measured three characteristics consistent with a fibrotic wound healing response: (1) increased expression of TGF β 1, a key regulator of wound healing and fibrosis, (2) gene expression profiles consistent with myofibroblast activation, with increased proliferation at the site of obstruction, and (3) evidence of stromal remodeling.

Our findings support a model where prenatal UPJ obstructions may be caused by an impaired urothelial barrier that allows urine to permeate and damage tissues lining the lumen, inducing a fibrotic wound healing response.

Table of Contents

Acknowledgments	i
Abstract	ii
List of Tables	iv
List of Figures	v
Introduction	1
Hydronephrosis and Clinical Relevance.....	1
Urinary System, Ureter and Urothelium Structure.....	2
Urinary Tract Development.....	5
Differentiation of Urothelium	7
The Exocyst	11
Sec10 Conditional Knockout Mouse Model.....	13
Hypotheses.....	13
Materials and Methods	15
Animals.....	15
Histology and Immunohistochemistry.....	16
Quantitative real time PCR analysis.....	17
Results	19
Sec10-CKO mice develop UPJ obstructions and hydronephrosis by E18.5	19
Sec10-CKO mouse ureters fail to develop a mature urothelial barrier.....	22
Sec10-CKO mouse ureters have impaired differentiation of urothelial cell layers	26
Sec10-CKO mouse ureters undergo a fibrotic wound-healing starting at E17.5.....	31
Discussion	38
Summary of Findings	38
Why is the UPJ a Hotspot for Obstructions?	38
Consequence of Urine Exposure to Interstitial Tissues of the Ureter	39
Intraluminal Wound Healing as an Underlying Mechanism of Obstruction	39
Comparison of the Sec10-CKO to other Mouse Models	43
Significance and Clinical Relevance	51
Conclusion.....	52
References	54

List of Tables

Table 1. Primer sequences used for real time qPCR.....	17
Table 2. Anneal and melt temperatures for each qPCR primer set.....	18
Table 3. Summary of knockout mouse models for congenital ureter obstruction.....	44
Table 4. Summary of other knockout mouse models for genes of interest.....	45

List of Figures

Figure 1. UPJ obstruction is the leading cause of prenatal hydronephrosis	1
Figure 2. Structure of Mature Ureter Urothelium	2
Figure 3. Uroplakin plaque assembly and trafficking.	4
Figure 4. Urothelial development in the mouse ureter.....	8
Figure 5. The exocyst complex.....	12
Figure 6. Generation of conditional Sec10 knockout mice.....	20
Figure 7. Sec10 ^{FL/FL} ;Ksp-Cre mice develop an obstruction in the ureteropelvic junction (UPJ) and hydronephrosis by E18.	22
Figure 8. Ureter urothelial cells lacking Sec10 expression disappear during development and do not contribute to the cell population forming the UPJ obstruction.....	23
Figure 9. Sec10 ^{FL/FL} ;Ksp-Cre mice have a leaky urothelial barrier at E17.5	24
Figure 10. Sec10 ^{FL/FL} ;Ksp-Cre mice have decreased tight junctions in the urothelium at E17.5	25
Figure 11. Sec10 ^{FL/FL} ;Ksp-Cre mice have no detectable uroplakins at E17.5	26
Figure 12. Sec10 ^{FL/FL} ;Ksp-Cre ureters have decreased transcription of uroplakins.....	28
Figure 13. Sec10 ^{FL/FL} ;Ksp-Cre ureter urothelial cells fail to differentiate	29
Figure 14. Sec10 ^{FL/FL} ;Ksp-Cre urothelial basal and intermediate cells begin to disappear at E17.5	31
Figure 15. Sec10 ^{FL/FL} ;Ksp-Cre mice develop an obstruction in the ureteropelvic junction (UPJ) by E18.5. from over-proliferation of SMA ⁺ cells.....	32
Figure 16. Sec10 ^{FL/FL} ;Ksp-Cre UPJ ureter obstructions are likely due to myofibroblast activation	34
Figure 17. Sec10 ^{FL/FL} ;Ksp-Cre UPJs have increased TGFβ1 expression at E17.5.	35
Figure 18. Sec10 ^{FL/FL} ;Ksp-Cre UPJ ureter obstructions have dysregulation of ECM deposition and basement membrane organization	37

Introduction

In this study, we investigated the role of the exocyst in the development of congenital abnormalities of the ureter.

Hydronephrosis and Clinical Relevance

The most common abnormality detected by prenatal ultrasounds is hydronephrosis: detected in 2.3% of fetuses (Sairam, et al. 2001) and possibly up to 7.7% (Gunn, Mora, and Pease 1995). Hydronephrosis is the swelling of the kidney when urine is prevented from passing into the ureter and bladder, distending the renal pelvis. Approximately 10-30% of hydronephrosis is caused by an obstruction of the ureteropelvic junction (UPJ), the superior region of the ureter where it transitions from the renal pelvis of the kidney (Nguyen, et al. 2010), as illustrated in Figure 1. About 1 in 6 cases of children born with hydronephrosis have bilateral obstructions (Livera, et al. 1989). Congenital obstructive uropathies, such as UPJ obstruction, account for 16.1% of children with end-stage renal disease (Benfield, et al. 2003).

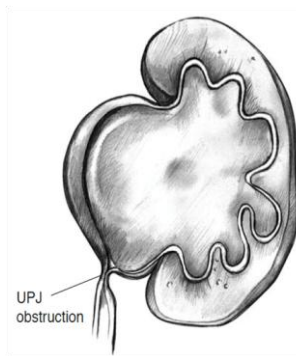


Figure 1. UPJ obstruction is the leading cause of prenatal hydronephrosis

Image is public domain (*Urine Blockage in Newborns*. 2006).

While 72-88% of prenatal hydronephrosis spontaneously resolves by 9 months after birth, (Gunn, Mora, and Pease 1995; Sairam, et al. 2001), 4.8% of fetuses with hydronephrosis detected at 18-23 weeks of gestation eventually require postnatal surgery (Sairam, et al. 2001). In the case of non-transient UPJ obstruction, surgical removal of the obstruction, pyeloplasty, is the only treatment option currently available.

Based on the number of births in the United States (www.cdc.gov/nchs/fastats/births.htm), it can be estimated that hydronephrosis is detected in over 90,000 fetuses annually with over 4,000 requiring surgical intervention shortly after birth. On a local level, it can be estimated that hydronephrosis is detected in over 400 fetuses annually in the state of Hawaii, with approximately 20 requiring surgical intervention, based on the number of births in 2015 (<http://health.hawaii.gov/vitalstatistics/preliminary-2015/>).

Urinary System, Ureter and Urothelium Structure

The kidneys filter the blood and produce urine to be excreted from the body. Urine flows from each kidney through a ureter to the bladder, where it is stored until it is expelled from the body through the urethra. The urinary tract is lined with a unique type of epithelium, termed the urothelium, which protects tissues from the toxic and damaging components of urine.

Urothelium is a stratified epithelium that allows for stretching, due to changes in urine volume, without compromising the impermeable barrier between the urine and the underlying tissues.

The urothelium is composed of three main cell layers: superficial, intermediate, and basal (Bohnenpoll and Kispert 2014). Superficial cells, also called umbrella cells, are the lumen-facing cells that are highly specialized to create a barrier impermeable to urine. Several rows of intermediate cells underlie the superficial cells. Basal cells form a single row of cells attached to the basement membrane.

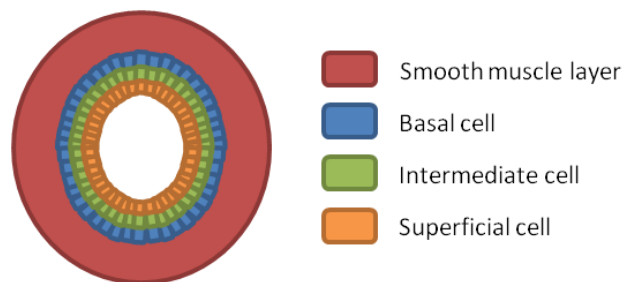


Figure 2. Structure of Mature Ureter Urothelium

The progenitor population of the adult urothelium used for regeneration is located in the intermediate layer (Gandhi, et al. 2013). Mature urothelium is considered quiescent due to its

slow turnover rate (Jost 1986), but retains high regenerative ability in response to injury through this progenitor population.

Superficial cells form specialized structures to provide a protective barrier from urine exposure, including tight junctions and uroplakin plaques. Urothelial cells utilize two main means of creating this barrier from urine: strong cell-cell adhesions and hydrophobic uroplakin plaque formation on the luminal plasma membrane.

Tight junctions (TJs) are specialized cell-cell adhesion proteins between neighboring cells at the apical pole, that prevent paracellular diffusion, and may have additional functions such as influencing cell polarity (Schneeberger and Lynch 2004). One study showed that knockdown of claudin 3, an important protein for TJ assembly, impaired barrier function in human urothelium (Smith, et al. 2015). Normal human urothelial cells were transfected with claudin 3 shRNA. These claudin 3 knockdown epithelia had significantly decreased transepithelial electrical resistance, a measure of TJ barrier “tightness,” compared to control epithelia.

Uroplakin plaques are hydrophobic structures unique to the urothelium that are critical to the formation of the functional urine barrier. The apical plasma membrane of the superficial cell is characterized by the presence of repeating plaques of asymmetric unit membrane (AUM), which is composed of uroplakins (UPKs) (Wu, et al. 1990), a family of highly conserved transmembrane proteins (Wu, et al. 1994).

Uroplakin plaque assembly starts with dimer formation between the four primary uroplakins: UPK1a dimerizes with UPK2, and UPK1b dimerizes with UPK3 (Wu, Medina, and Sun 1995). UPKs remain in the endoplasmic reticulum until these heterodimers have formed, although UPK1b can sometimes be trafficked to the plasma membrane as a monomer. The heterodimers then form heterotetramers, UPK1a/UPK2/UPK1b/UPK3, and multiple heterotetramers assemble to form hydrophobic uroplakin plaques, 16nm 2D crystals, in the trans-Golgi network (Tu, Sun, and Kreibich 2002). These rigid plaques are connected with flexible hinge regions that allow for stretch of the urothelium. Using mouse knock out studies of UPK gene members, it was shown that UPKs are critically important for barrier function in the urinary tract (Hu, et al. 2002).

Bladder urothelium studies indicate that exocytosis and endocytosis of uroplakins can increase or decrease luminal membrane, respectively, to accommodate changes in urine volume (Truschel, et al. 2002).

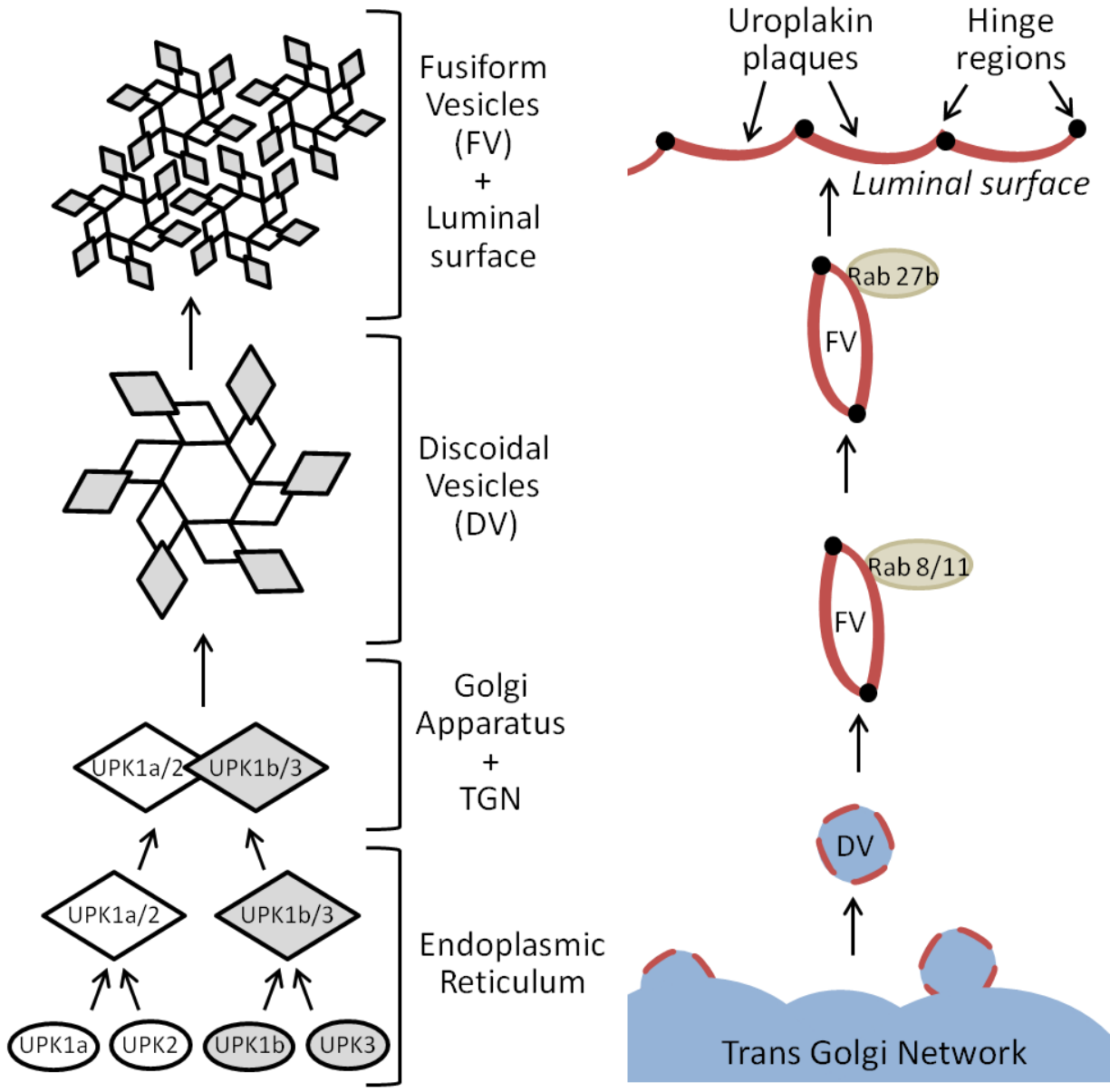


Figure 3. Uroplakin plaque assembly and trafficking.
 Diagram based on previous reports (Wankel, et al. 2016; Wu, et al. 2009)

Uroplakin plaques are trafficked to the plasma membrane in discoidal/fusiform vesicles; Rab8 (Wankel, et al. 2016), Rab11a (Khandelwal, et al. 2008) and Rab27b (Chen, et al. 2003) GTPases associate with these vesicles and are crucial for the exocytosis of uroplakin plaques at the apical plasma membrane. Recent findings suggest that each of the above mentioned Rab GTPases will act in sequence, and each play a role in trafficking within discrete regions (Wankel, et al. 2016). For example, Rab8 is crucial for trafficking fusiform vesicles within deeper regions of the cytoplasm; Rab27b is crucial for trafficking from within the more superficial cytoplasm to the apical membrane, and also for SNARE-mediated fusion to the plasma membrane.

Urinary Tract Development

During mammalian development, the kidney develops in three stages following the formation of two nephric (or Wolffian) ducts from the intermediate mesoderm: (1) the pronephros is the first set of kidneys to develop at the cranial portion of the nephric duct and is derived from the intermediate mesoderm at embryonic day 8 (E8) in mice; the pronephros is non-functional in mammals and eventually degenerates. (2) the mesonephros develops caudal to the pronephros and is derived from the aorta-gonad mesonephros zone of the mesoderm; the mesonephros is briefly functional in some mammals including humans, but not in others including mice, and is subsequently degenerated. (3) the final kidney, metanephros, forms when the ureteric bud (UB) emerges from the caudal region of the nephric duct (also called the mesonephric duct or Wolffian duct), before the duct fuses to the cloaca. In mice, the metanephros begins to develop at E10.5, with the sprouting of the UB. (Kuure, Vuolteenaho, and Vainio 2000)

The pronephros is non-functional in mammalian embryos; this structure develops in all vertebrates and is the final kidney in some fish (Seufert, et al. 1999). The mesonephros is briefly functional in some mammals including humans, but not in others including mice; the mesonephros forms the final kidney in most fish and amphibians (Diep, et al. 2015). Both the pronephros and mesonephros degenerate in amniotes and are replaced by the metanephric kidneys (Davidson 2008).

The sequential development of these structures in embryo development is reminiscent of vertebrate evolution and the increasing complexity of each subsequent kidney reflects the

growing requirements for efficient filtration; increased water retention allows for life on land (Smith 1959).

During normal development, embryos develop a right and left nephric duct (ND), which are the epithelial tubes that give rise to critical structures of the adult urogenital system. A single UB epithelial tube buds off from each nephric duct, directed by signals from the adjacent metanephric mesenchyme (MM). The MM secretes glial cell line-derived neurotrophic factor (GDNF), which stimulates the receptor tyrosine kinase Ret on the UB epithelial cells to regulate ureteric budding. Neighboring mesenchymal cells that do not belong to the MM inhibit GDNF/Ret signaling through Bmp4 expression. These three cell types each regulate each other to ensure a single UB is formed from each ND (Dressler 2009). Since the stalk of the UB develops into the ureter, these signaling events are crucial to the formation of a single ureter; multiple UBs can result from enhanced GDNF/Ret signaling, ultimately leading to additional ureters (Bohnenpoll and Kispert 2014). Once the UB enters the MM, the UB tip undergoes branching, which will ultimately form the collecting ducts of the kidney. After the UB invades the MM and begins branching, the UB expresses Wnt9b which signals for the condensation of the MM at the tips of the UB (Dressler 2009). Budding of the UB is initiated by signals from the MM and condensation of MM is signaled from the UB; these examples illustrate that the UB plays a role in MM development and the MM on UB development, respectively. Throughout the development of the urinary system, there are multiple instances of similar mesenchymal-epithelial interactions underlying complex patterning events.

While the collecting system of the kidney and the ureter is lined with urothelia derived from the UB, other organs of the urinary system (i.e. bladder and urethra) are lined with urothelia derived from cells of a different lineage: the endodermal urogenital sinus (Rasouly and Lu 2013). Therefore, studies on bladder urothelial development may or may not be consistent with the urothelial development of the ureter. This is an important point for consideration in our study since most previous studies of urothelial differentiation come from investigations of bladder development.

Differentiation of Urothelium

The portion of the UB that does not enter the MM (the UB stalk) will continue to differentiate to form the ureter (Bohnenpoll and Kispert 2014). Ureter formation requires recruitment of mesenchyme to surround the UB. This mesenchymal coat differentiates around E15.5 into two main cell types: (1) smooth muscle cells, required for the structural strength and flexibility of the ureter and for peristalsis, which starts around E16.5, and (2) fibroblasts, which develop into the tunica adventitia and the lamina propria. The UB cells will differentiate into multilayered urothelium.

The term “urothelium” refers to the epithelial lining of the urinary tract. However, urothelia of the (1) renal pelvis/ureter, (2) bladder/trigone and (3) proximal urethra are derived from three distinct embryonic origins. Differences in developmental origin may manifest in structural differences between these three groups. For example, uroplakin protein content is ten times greater in bladder compared to ureter urothelia, as measured with immunoblotting (Liang, et al. 2005). The amount of uroplakin is very dynamic. The bladder likely requires more uroplakins due to the higher hydrostatic pressure it experiences; hydrostatic pressure causes cells to stretch and increase surface area of the apical membrane. Since bladder cells will need to stretch more than ureter cells, bladder urothelium will require more uroplakins to be available to cover the additional apical membrane. It is possible these differences in structure and origin will also entail different signaling events that regulate development and differentiation.

In the bladder, urothelium development starts with the appearance of transient progenitor urothelial cells (P cells), detected from E11 to E13. P cells generate intermediate and superficial cells. Intermediate cells retain this regenerative potential and serve as progenitors for superficial cells (Gandhi, et al. 2013). It is not clear whether basal cells, which form last, are derived from intermediate cells, from another cell population, or if they are self-renewing (Yamany, Van Batavia, and Mendelsohn 2014).

We found that the development of the UPJ region of the ureter is generally consistent with other descriptions of ureter development (Bohnenpoll and Kispert 2014). Figure 4 illustrates the timeline of urothelial differentiation in the ureter. At E16.5, there is a thickening of the

urothelial monolayer, with early stratification evident at E17.5. Ureter urothelium is fully differentiated by E18.5.

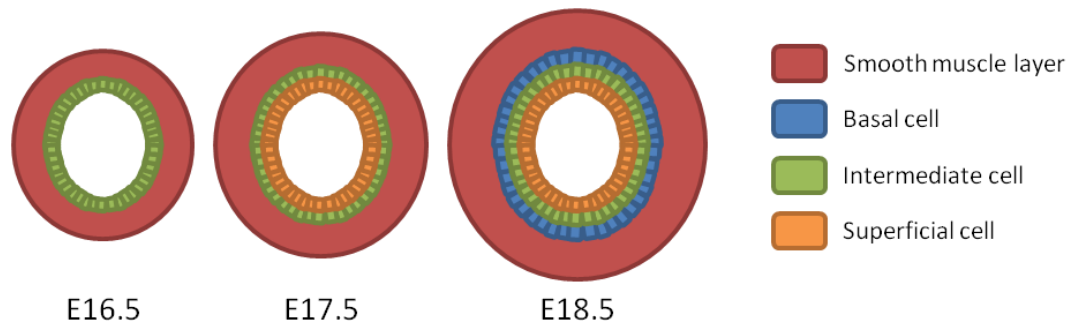


Figure 4. Urothelial development in the mouse ureter

As with the development of the kidney, critical signaling events regulating ureter tissue differentiation originate from two key tissue types: mesenchymal and epithelial (urothelial) signaling.

Mesenchymal signaling regulates urothelial development:

Retinoic acid (RA) signaling controls specification of P cell as progenitors in development, and intermediate cell as progenitors during regeneration (Gandhi, et al. 2013). In the bladder of mice, RA synthesis is believed to occur in the underlying mesenchyme, indicating P cells and intermediate cell differentiation is likely signaled by the surrounding smooth muscle cells. Inhibition of RA signaling in urothelial cells during development results in no UPK expression, marking defective superficial cell differentiation (Gandhi, et al. 2013).

T-box18 (Tbx18) is a transcription factor expressed in the metanephric mesenchyme destined to condense around the ureter, and in the mesenchymal cells that ultimately form the machinery for ureter peristalsis. Tbx18 is required for normal differentiation of both the smooth muscle cells and urothelium of the ureter (Airik, et al. 2006). Interestingly, Tbx18 is only expressed in the ureter and is not expressed in any other component of the urogenital system between E12.5 and E14.5. This is significant because the urothelial development of the ureter occurs later than in the bladder. Because Tbx18 signaling is unique to ureter epithelium, it may

provide an interesting explanation as to why urothelial differentiation is delayed or slower in the ureter than in the bladder.

Urothelial signaling regulates mesenchymal development:

Wnts are expressed in ureteric epithelia, including Wnt7b and Wnt9b, and ureteric mesenchyme express the Wnt receptor frizzled (Fzd). Canonical Wnt signaling activates proliferation of mesenchyme and smooth muscle development (Trowe, et al. 2012).

Sonic hedgehog (Shh) is expressed in the ureteric epithelium from E11.5 to E18.5. Ureteric mesenchyme expresses the Shh receptor, *patched homolog1* (Ptch1). Paracrine Shh activity is known to signal differentiation of smooth muscle cells (Yu, Carroll, and McMahon 2002).

Smooth muscle cell differentiation program is signaled through Shh, and mediated by Bmp4 and downstream target *teashirt3* (Tshz3), subsequently recruiting the transcription factor Myocd to activate smooth muscle-specific gene expression pattern. In one study, mice lacking Tshz3 developed hydronephrosis secondary to defective smooth muscle differentiation, not due to a physical obstruction (Caubit, et al. 2008).

Urothelial signaling regulates its own development:

Peroxisome proliferator-activated receptors (PPARs) are intracellular transcription factors. Binding of ligands, such as the prostaglandin metabolite 15d-J2, activates PPARs (Qi, Zhu, and Reddy 2000), which then heterodimerize with retinoid X receptor (RXR) (Keller, et al. 1993); this complex binds to peroxisome proliferator response elements (PPRE) located in the promoter of target genes (Kliwer, et al. 1992). mRNA expression of the PPAR γ isoform is detectable in urothelial cell types of the developing ureter epithelium at E13.5. This expression is upregulated in the superficial cells as the monolayer stratifies between E14.5 and E16.5 (Weiss, et al. 2013).

PPAR γ is a critical regulator of urothelial differentiation. Conditional PPAR γ knockout experiments from UB derived epithelial tissues result in healthy mice up to 26 weeks. However, histological analyses of the PPAR γ knockout urothelium showed (1) a decrease in superficial cell markers, (2) decreased Shh expression, and (3) abnormal basal cell layer infoldings, likely due to increased p63 expression (Weiss, et al. 2013). This suggests PPAR γ is not only critical for

superficial cell differentiation, but may also be important for smooth muscle differentiation and may suppress proliferation of urothelial progenitors.

PPAR γ induces expression of several genes important for terminal urothelial differentiation including UPK1a, UPK1b and UPK2. However, no PPRE binding sites have been identified in UPK promoters, indicating that PPAR γ does not have direct transcriptional activation of UPK expression (Varley, et al. 2004). Instead PPAR γ activation induces expression of FOXA1 and IRF1, two transcription factors that directly induce genes associated with urothelial differentiation, including the UPK gene family (Varley, et al. 2009).

Epidermal growth factor receptor (EGFR) signaling regulates urothelial proliferation (Varley, et al. 2005), while PPAR γ suppresses proliferation of basal urothelial cells (Kawakami, et al. 2002). PPAR γ -induced terminal urothelial differentiation is amplified when EGFR signaling is concurrently inhibited (Varley, et al. 2004). This interplay may explain why urothelium is largely quiescent, but following injury EGFR can facilitate rapid proliferation for regeneration.

ELF3, a critical regulator of urothelial differentiation, is upregulated in response to PPAR γ . ELF3 plays a role in the establishment of the functional barrier, by upregulating UPK3a transcription, and is critical for barrier repair following injury (Bock, et al. 2014) or infection (Mysorekar, et al. 2002).

Brg1 acts upstream of PPAR γ . Brg1 is a critical member of the Switch/Sucrose non-fermentable (Swi/Snf) complex that is essential for maintenance of stem cell pluripotency and renewal during development (Bultman, et al. 2000). Swi/Snf, a chromatin remodeling complex, is a global transcriptional activator (Carlson and Laurent 1994). Brg1 is highly expressed in developing ureter epithelium from E12.5-E16.5 (Bohnenpoll and Kispert 2014). Brg1 null ureters have a detectable reduction in smooth muscle development by E16.5, likely mediated by diminished Shh expression, and decreased p63 expression (Weiss, et al. 2013).

p63 is critical for proliferative self-renewal of stem cells in stratified epithelia (Senoo, et al. 2007). In Brg1 null ureters, epithelium fails to stratify due to the loss of Brg1-induced expression of p63 (specifically the Δ Np63 isoform) (Weiss, et al. 2013).

The Exocyst

The exocyst is a highly conserved protein complex made up of a single copy of eight subunits: Sec 3 (also known as EXOC1), Sec5 (EXOC2), Sec6 (EXOC3), Sec8 (EXOC4), Sec10 (EXOC5), Sec15 (EXOC6), Exo70 (EXOC7), and Exo84 (EXOC8). This complex associates with and traffics a subset of secretory vesicles. The exocyst is recruited to sites of membrane expansion and functions as the tether between the secretory vesicle and the plasma membrane. The involvement of the exocyst allows for soluble N-ethylmaleimide-sensitive factor attachment protein receptor (SNARE) to mediate membrane fusion of the tethered secretory vesicles (Wu and Guo 2015) .

In epithelial cells, the exocyst trafficking of vesicles can be directed to several regions of the plasma membrane. Small GTPases, including Rabs, Rals and Rhos, are known to regulate exocyst trafficking. Rab proteins on the surface of the secretory vesicle interact with Sec15 and play a role in the regulation of where the exocyst traffics these vesicles (Wu and Guo 2015). Sec15 binds to certain Rab GTPases on secretory vesicles; currently, Rab3, Rab8, Rab11 and Rab27 are confirmed to interact with Sec15 (Wu and Guo 2015). For example, Rab11a facilitates trafficking to the apical domain for Par3, a critical regulator of polarity (Bryant, et al. 2010). Members of the Ral family of small GTPases can also regulate the exocyst; RalA and RalB regulate exocyst-mediated tight junction formation (Hazelett, Sheff, and Yeaman 2011). Rho GTPases Cdc42 and Rho1 compete to bind to Sec3 to regulate exocytosis to establish and maintain cell polarity (Zhang, et al. 2001).

Sec10 is a central unit of the complex and acts as the “linker” that connects Sec15 to the rest of the exocyst complex (Guo, et al. 1999). When Sec10 is knocked down in mammalian epithelial cells, other exocyst subunits degrade, and furthermore there is decreased exocyst trafficking activity (Zuo, Guo, and Lipschutz 2009).

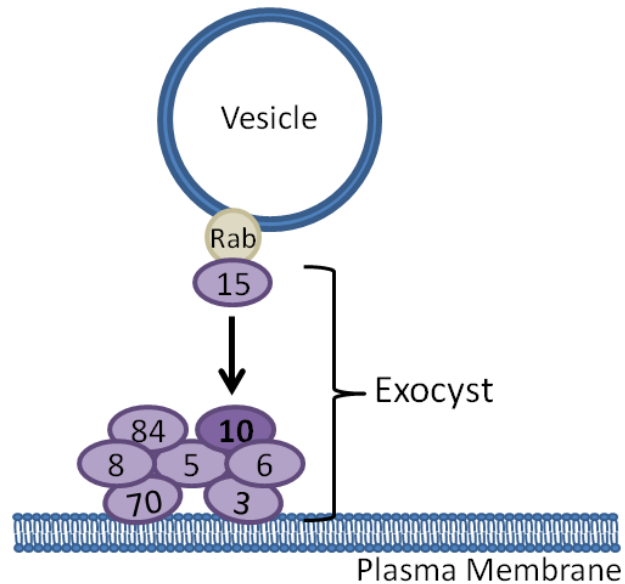


Figure 5. The exocyst complex

We are interested in the role of the exocyst in the development and physiology of the epithelial tissues of the urinary system.

It is already known that the exocyst traffics important adhesion proteins in epithelial cells: E-cadherins (Langevin, et al. 2005) and products important for desmosome assembly (Andersen and Yeaman 2010) to the basolateral membrane. Additionally, the exocyst has been found to localize to primary cilia (Rogers, et al. 2004) where it traffics ciliary proteins (Zuo, Guo, and Lipschutz 2009). Progenitor, but not mature, urothelial cells have primary cilia which serve as a sensory organelle to regulate cell function (our unpublished data), but there have been no reports of possible ciliary function in these cells.

During the course of this study, we found that global knockout of Sec10 in mice is embryonic lethal sometime prior E8.5 (Fogelgren, et al. 2015), indicating the exocyst is critical for early fetal development. This is consistent with results of knock-out experiments for other exocyst subunits, which were lethal to developing *Drosophila* larvae (Murthy, et al. 2003; Murthy, et al. 2005) and embryonic lethal in mice (Friedrich, Hildebrand, and Soriano 1997).

Sec10 Conditional Knockout Mouse Model

To study the effects of Sec10 urothelial development, we generated a conditional knock out mouse. We designed a floxed Sec10 mouse strain (Sec10^{F1/F1}), where exons 7-10 are flanked by loxP sites, such that Cre-recombinase expression can be used to excise these exons and the resultant Sec10 transcripts will have a premature stop codon (Fogelgren, et al. 2015). In the Ksp1.3-Cre mouse strain, Cre-recombinase expression is driven by a 1.3 kb fragment of the Ksp-Cadherin promoter region. Ksp-cadherin expression is tissue-specific and can be detected in epithelial cells derived from the nephric duct (Shao, Somlo, and Igarashi 2002).

Breeding the Sec10^{F1/F1} mice strain with the Ksp-Cre mouse strain allowed us to generate a conditional Sec10 knockout (Sec10^{F1/F1};Ksp-Cre). These mutant offspring have severe bilateral hydronephrosis caused by complete obstruction of the UPJ region by E18.5, complete anuria at birth, and death by 14 hours after birth (Fogelgren, et al. 2015).

The aim of this study is to better understand the process of prenatal UPJ obstruction development in these Sec10 conditional knockout mice, as compared to normal ureter development.

Hypotheses

We have previously shown that knockout of Sec10 from the developing mouse urothelium results in severe bilateral hydronephrosis secondary to obstruction at the UPJ region (Fogelgren, et al. 2015).

We hypothesize that the exocyst is required for the development of a mature urothelial barrier that prevents urine leakage. The exocyst contributes to the formation of cell-cell adhesions (Hazelett, Sheff, and Yeaman 2011), and may traffic uroplakins to the plasma membrane. We hypothesize that barrier permeability and obstructive phenotype will be more severe than in knockout mouse models of either uroplakins or tight junctions alone.

Ureter development requires complex signaling between different tissues. It is possible that a critical signaling event may require exocyst function for exocytosis of the signal or for trafficking

receptors to the plasma membrane. We hypothesize that urothelial cells will fail to differentiate normally in the absence of exocyst function.

We hypothesize that luminal damage will initiate a fibro-proliferative wound healing response that obstructs the lumen. If the urothelial barrier is leaky, then underlying tissues will be exposed to urine following the start of urine production at E16.5 (Bohnenpoll and Kispert 2014). The cytotoxic effect of urine may initiate a wound healing response with granulation tissue formation, which includes activation of myofibroblasts at the site of injury and stromal remodeling.

Materials and Methods

Animals

All animal procedures and protocols were carried out in accordance with IACUC specifications approved by the University of Hawaii Animal and Veterinary Services. Dr. Fogelgren's IACUC approved protocol is #11-1094, and the University of Hawaii has an Animal Welfare Assurance on file with the Office of Laboratory Animal Welfare (OLAW), assurance number is A3423-01. Adult mice were housed under standard conditions with 12-hr light cycle and supplied with water and food *ad libitum*. The floxed *Sec10* (ie. EXOC5) mouse strain (*Sec10^{FL/FL}*) was generated as previously described (Fogelgren, et al. 2015). Briefly, we obtained from the trans-NIH Knock-Out Mouse Project (KOMP) repository an Embryonic Stem (ES) cell clone which contains loxP sites flanking *Sec10* exons 7–10. The ES clone was injected into blastocysts (albino C57Bl/6J) to generate chimeras with germline transmission.

We designated the final mouse strain the floxed-*Sec10* line. Using a Cre-lox system, we achieved the conditional knock out of *Sec10* exons 7–10 in epithelia derived from the ureteric bud by mating this floxed-*Sec10* line with Ksp1.3-Cre mice, obtained from Jackson Laboratories (Shao, Somlo, and Igarashi 2002; Shao, et al. 2002).

The *B6.Cg-Gt(ROSA)26Sor^{tm9(CAG-tdTomato)Hze/J}* reporter mouse strain (here designated *tdTomato* or *To*) was kindly provided by Dr. Michelle Tallquist at University of Hawaii and was used to detect Cre recombinase activity through Cre-activated expression of the tdTomato red fluorescent protein (Madisen, et al. 2010).

All mice were of C57Bl/6J inbred background. For timed matings, mice mated overnight were examined for a vaginal plug the following morning and constituted gestational day E0.5 if present. Both male and female embryos were obtained between days E16.5 and E18.5 and were subsequently staged using Theiler staging criteria (TS) to ensure the developmental stage of each embryo was similar to the conception day (E) designation (Theiler 2013). Only animals of the same E designation and TS were compared.

Histology and Immunohistochemistry

Caudal torsos of Sec10 knockout and control animals were dissected, the abdominal cavity opened, immediately placed in freshly prepared 4% formaldehyde in PBS, and fixed overnight with rocking at 4°C. Some samples were embedded in paraffin according to standard methods, and some samples were instead were frozen in OCT and subjected to cryosectioning. The tissues were sectioned into 5 µm sections and stained.

For immunostaining, tissue sections were deparaffinized, rehydrated in an ethanol gradient, and placed in a pressure cooker for antigen retrieval with citric acid based antigen-unmasking solution (Vector Laboratories H-3300). Sections were blocked with 5% serum, permeabilized with 0.1% Triton X-100, and left in primary antibody overnight at 4°C.

Primary antibodies used for immunostaining were: anti-Ki67 at 1:200 (Cell Signaling); anti-E-cadherin at 1:200 (Cell Signaling Tech.); anti-p63 at manufacturer's prepared dilution (Biocare Medical); anti-collagen IV at 1:200 (Abcam); (Cell Signaling Tech.); UPK1a at 1:200 (Santa Cruz); UPK1b at 1:200 (Sigma-Aldrich); UPK2 at 1:200 (Santa Cruz), UPK3 at 1:200(American Research Products, Inc.); anti-smooth muscle actin at 1:800 (Sigma).

Tissue sections were washed and incubated with DyLight secondary antibodies (Vector Laboratories) for 1 hour at room temperature. Nuclei were stained with DAPI.

H&E stained and immunostained sections were analyzed using a fluorescent Olympus BX41 microscope or an Olympus Fluoview1000 confocal microscope. Image processing, quantification of cell counts were performed using Image J software (NIH).

For ureter injections, fluorescein isothiocyanate (FITC) labeled dextran (average molecular weight 10,000, Cat # FD10S, Sigma) was dissolved in PBS to make a stock solution of 25 mg/ml. The FITC-dextran solution was injected into the renal pelvis (left kidney only) of genitourinary tracts and allowed to flow to the bladder. Injected tissues were frozen in OCT, cryosectioned, dried, and analyzed with a fluorescent Olympus BX41 microscope.

Quantitative real time PCR analysis

Ureter segments from the UPJ region from embryos of various stages were dissected and placed immediately into RNAlater (Sigma) and stored at -20°C. RNA was extracted from these samples in one of two ways: (1) Pooled samples: RNA was extracted from UPJ regions from three animals of the same stage and with the same genotype that were pooled together, using the RNeasy micro kit (Qiagen), or (2) Individual samples: RNA was extracted from UPJ regions from each individual mouse separately, using the Direct-zol RNA MicroPrep (Zymo Research).

cDNA was generated from extracted RNA using the iSCRIPT reverse transcriptase (Bio-Rad) and qPCR was performed using SYBR green (Bio-Rad) with a CFX96 Real TimeSystem (Bio-Rad), as per the manufacturer's recommended instructions. Refer to Table #1 for a complete list of primer sequences used for qPCR. Each primer set was selected from previous published works.

Table 1. Primer sequences used for real time qPCR.

Gene	Forward Primer (5'-3')	Reverse Primer (5'-3')
Collagen IV	TCCAGGCCCCCTGGAAGTGT	GAGGGCCTGGTTGGCCTG
Desmin	ACCTTCTCTGCTCTCAACTTCC	CGCTGACAACCTCTCCATCC
ED-A FN	GCAGTGACCAACATTGATCGC	ACCCTGTACCTGGAAACTTGCC
Periostin	GAATGGTGTATCCACCTGA	GTCCATGCTCAGAGTGTCAT
PPAR γ	GGAGTTCATGCTTGTGAAGG	CCTGATGGCATTGTGAGACA
S100A4	CAGGCAAAGAGGGTGACAAG	CAATGCAGGACAGGAAGACA
TGF-Beta	AGGGCTACCATGCCAAGTTC	CCACGTAGTCGATGGGC
Upk1a	AGGCAAGGATGATGTCTTCG	ATGAGCATCAGCAGCAGGTA
Upk1b	CTTGATAGGCATGTTTCGTG	CTGTGATGCAAGATGCCACT
Upk2	ATCCTGATTCTGCTGGCTGT	GGACACCACAAAGTCTGACTT
Upk3a	CGGCCACTGAGTACAGATTC	GGACGTGATGACAATCATGC

The PCR reaction starts with 3 minutes of denaturation at 94°C. Reaction cycles consist of a denaturation step (15 seconds at 95°C), followed by an annealing step (15 seconds at the anneal temperature for the primers used; see Table #2), then an elongation step (30 seconds at 72°C), and concludes with a plate read (8 seconds at the melt temperature for the primer set used). We used 40 cycles to amplify PCR products.

Table 2. Anneal and melt temperatures for each qPCR primer set.

qPCR Primers	Anneal Temp	Melt Temp
B-actin	55	80
Collagen IV	64	79
Desmin	59	76
ED-A	61	76
PPAR γ	52	74
S100A4	54	78
TGFb	64	81
TNFa	61	78
UPK1a	55	80
UPK1b	55	74
UPK2	55	80
UPK3a	55	82
UPK3b	55	82

Anneal temperatures for each primer were determined by running PCR amplification at several temperatures to determine which temperature yields products that, when run on an agarose gel, form a single band of the predicted size.

Gene expression in embryonic tissues using real time quantitative PCR (qPCR) was performed using the 2^{-Ct} method of analysis to calculate fold changes of expression (Fogelgren, et al. 2009). The mRNA expression levels of genes of interest in each sample were compared to β -actin expression, with the relative ratio of a representative E15.5 wildtype sample set to 1.

Differences between means for any parameter measured in two groups of age-matched mice were evaluated using Student's t-tests. Expression data was analyzed using Graphpad Prism software.

Results

Sec10-CKO mice develop UPJ obstructions and hydronephrosis by E18.5

To study the effect of disruption of exocyst function in urinary tract development, we generated a floxed-*Sec10* ($Sec10^{FL}$) mouse strain such that the *Sec10* gene would have critical exons excised when exposed to Cre recombinase (Figure 6A). Kidney-specific protein (Ksp) is expressed only in cells derived from the nephric duct and ureteric bud. Therefore, Ksp-Cre mice primarily express Cre recombinase in epithelia lining the kidney collecting system and ureters (Shao, Somlo, and Igarashi 2002). When $Sec10^{FL/FL}$ mice mate with $Sec10^{FL/+};Ksp-Cre/+$ mice, it is expected 25% of their offspring will be $Sec10^{FL/FL};Ksp-Cre$ mice, following Mendelian ratios. $Sec10^{FL/FL};Ksp-Cre$ mice have a conditional knockout (CKO) of *Sec10* in kidney and ureter epithelia, and normal *Sec10* expression in all other tissues.

The specificity of the tissues with *Sec10* knocked out was confirmed using two methods. First, PCR products of genomic DNA extracted from various tissues, were run on an agarose gel. As shown in Figure 6B, the top panel confirms the animal genotype based on the size of the *Sec10* band: the added LoxP sites to the $Sec10^{FL}$ allele increase the size of the PCR amplicon, and is visible as a higher molecular weight band. The second panel shows detection of the Cre allele. In the third panel, we were able to detect Cre recombination with another set of primers, with a sequence that matches either size of the deleted loxP-flanked sequence. While all tissues of *Sec10*-CKO mice had bands for the floxed *Sec10* allele and for the Cre recombinase gene, only targeted tissues (kidney and ureter) had evidence of Cre recombination, required for inactivating the floxed *Sec10* allele (Figure 6B).

The second method used to confirm tissue specificity and timing of Cre-expression was with a cross between the Ksp-Cre mice and a transgenic reporter mouse strain that fluoresces red in cells where Cre is present. The Rosa26-tdTomato Cre-reporter mice do not express the Tomato gene unless exposed to Cre-recombinase (Madisen, et al. 2010). The Rosa26 gene has a “stop” codon flanked by loxP sites so when Cre is present, the stop codon will be excised and the tomato gene is expressed. As a result, the cell will have this red fluorescent protein. Therefore, whole mount images of the embryo will appear red only in cells with Cre-expression.

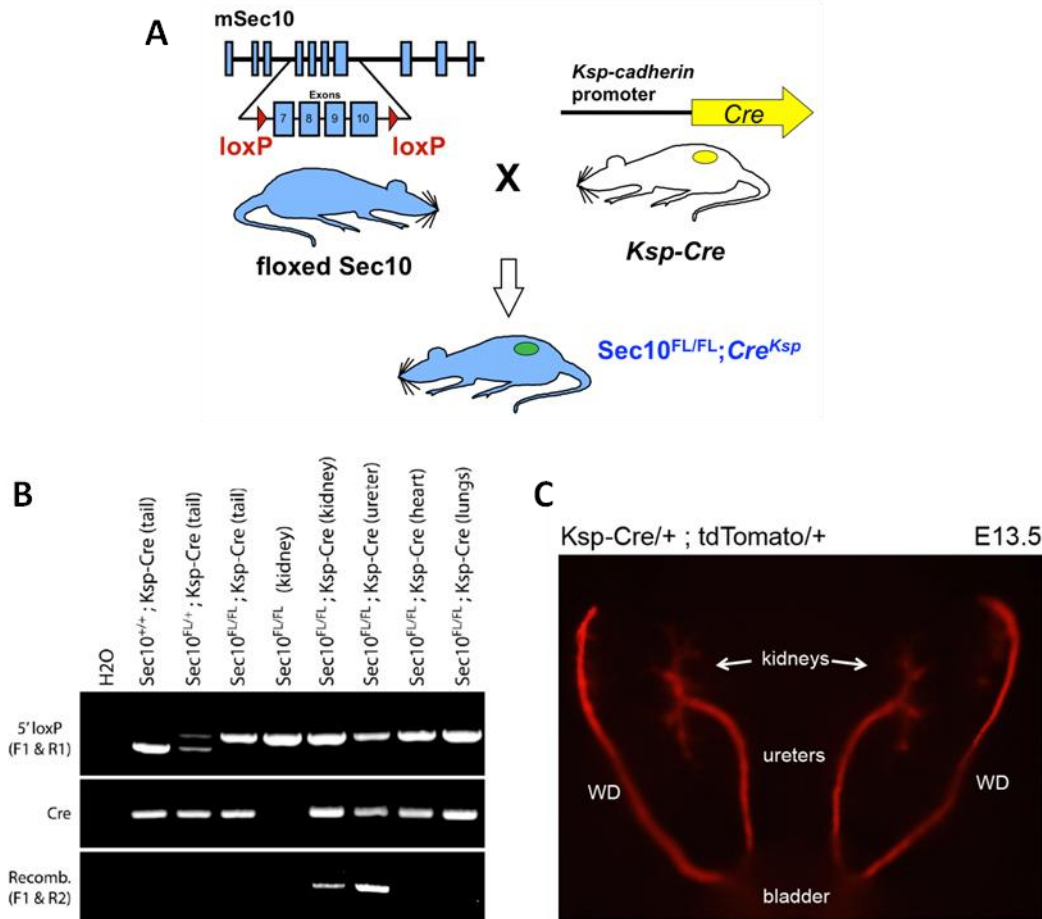


Figure 6. Generation of conditional Sec10 knockout mice

(A) We generated a floxed Sec10 mouse (Sec10^{FL}) mouse strain with loxP sites flanking exons 7 through 10. Sec10^{FL} mice mated with Ksp-Cre mice generate a conditional knock out of Sec10, only in the epithelium lining the kidney collecting system, ureters, and Wolffian ducts. (B) Genomic PCR products run on an agarose gel allowed us to genotype different animals and detect Cre deletion of Sec10 exons. The 5'loxP primer can be found in floxed Sec10 alleles (top band), and in wildtype Sec10 alleles (lower band). In this same way we were able to detect the presence of the Cre-recombinase allele, and also detect Cre-recombination products indicative of Sec10 knockout. Various tissues were genotyped, but only Sec10-CKO kidney and ureter tissues showed Cre-mediated recombination. (C) Ksp-Cre mice were crossed with a tdTomato reporter mouse strain confirmed Cre expression is specific to desired tissues. Imaging red fluorescence of the genitourinary system of E13.5 Ksp-Cre/+;tdTomato/+ embryos confirming strong activation of Cre recombinase to epithelium of ureters, Wolffian ducts (WD), and the collecting system of the kidney.

Sec10-CKO mice with the Rosa26-tdTomato allele bred in (Sec10^{FL/FL};Ksp-Cre/+;tdTomato), red fluorescence was specific to cells derived from the nephric duct, indicating Ksp linked Cre-expression is specific and does not leak into other tissues (Figure 6C). This image was collected from an E13.5 embryo, indicating that Cre-mediated recombination due to the Ksp-Cre allele is

robust by this time point. Previous reports were ambiguous on the timing of Ksp-Cre expression during embryonic development, and this was an important point to establish in our model system. For more information on the generation of this mouse model, see the Methods section of our publication (Fogelgren, et al. 2015).

We collected E18.5 and newborn embryos, surgically removed the urinary tract, and sectioned these tissues to analyze morphology. We used Sec10^{FL/FL} littermates as age-matched controls to compare with Sec10-CKO morphology. We chose the Sec10^{FL/FL} genotype as the control because the only difference between them and Sec10-CKO is Cre-expression. These control mice are phenotypically identical to wildtype mice, indicating the floxed Sec10 allele itself is functional until exposed to Cre-recombinase.

Tissue sections were stained with hematoxylin and eosin (H&E) to visualize the morphology of the urothelial cells. Hematoxylin stains nucleic acids and the nucleus a blue-purple color, while eosin stains proteins a pink color (Fischer, et al. 2008). Sagittal sections of the kidney (Figure 7A-B) show Sec10-CKO mice develop severe, bilateral hydronephrosis by embryonic day 18.5 (E18.5). Hydronephrosis can be caused by a structural obstruction, where there is a physical blockage, or a functional obstruction, where a defect in the smooth muscle layer impairs the conduction of fluid to the bladder. To determine which type of obstruction causes hydronephrosis in Sec10-CKO mice, we analyzed the morphology of the ureter with H&E staining. Cross sections of Sec10-CKO ureters (Figure 7C-D) show congenital obstructions at the ureteropelvic junction (UPJ). Dye injected into the renal pelvis of control mice migrated into the bladder in control mice, but failed to pass the UPJ region in Sec10-CKO mice (data not shown), confirming a physical obstruction (Fogelgren, et al. 2015).

This obstruction begins to form at E17.5 and we believe that the UPJ obstruction is the cause of hydronephrosis. None of the control mice developed hydronephrosis, ureter obstructions or malformations. As we previously published, this condition is neonatal lethal due to complete anuria and heart failure, with approximately 95% of Sec10-CKO mice dying within the first day after birth (Fogelgren, et al. 2015).

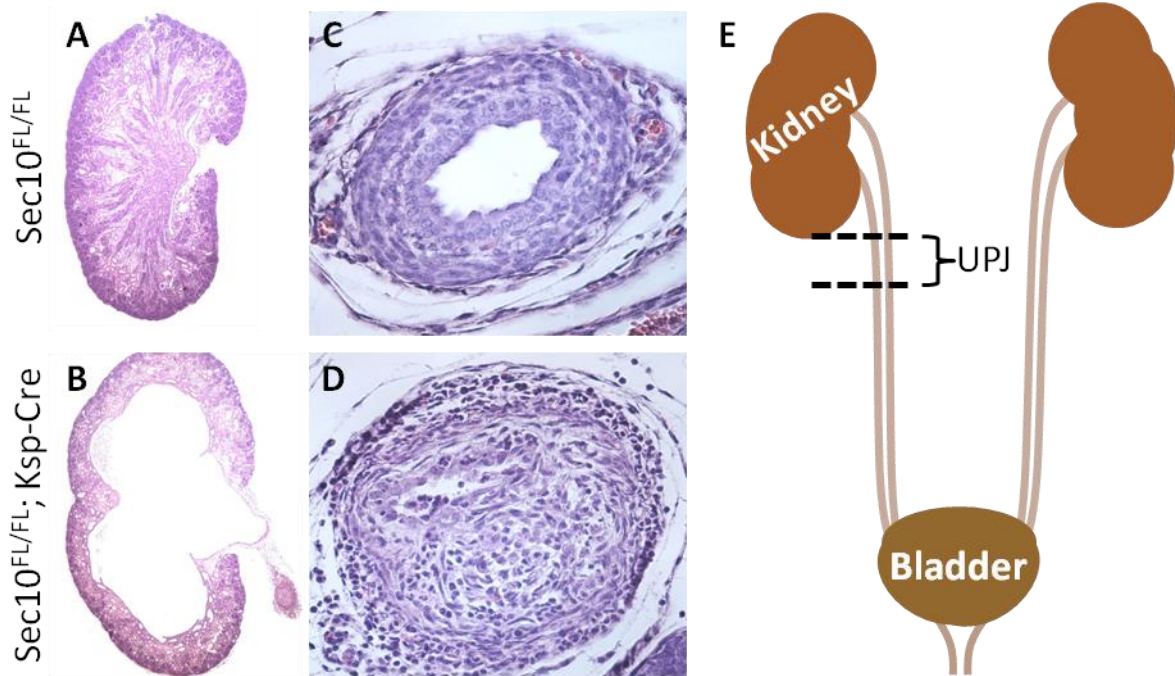


Figure 7. $Sec10^{FL/FL};Ksp-Cre$ mice develop an obstruction at the UPJ region and hydronephrosis by E18. (A, B) H&E sections of the E18.5 kidney revealed severe, bilateral hydronephrosis. (C, D) H&E sections of newborn ureters at the UPJ region revealed an obstruction. (E) This diagram illustrates the portion of the ureter defined as the UPJ: the superior border of the UPJ is defined by the base of the ipsilateral kidney. The H&E section and future tissue analyses of the UPJ refer to this region.

Sec10-CKO mouse ureters fail to develop a mature urothelial barrier

Histological analyses showed that a population of mesenchymal-appearing cells made up the UPJ obstruction in Sec10-CKOs. To determine the cellular basis of the obstruction, we conducted histological analyses on cross sections of embryonic UPJs. Using immunohistochemistry, we were able to mark the specialized epithelium that lines the urinary tract: urothelium. Similar to all epithelia, urothelial cells express E-Cadherin, while the surrounding smooth muscle cells express smooth muscle actin (SMA). By fluorescently staining for E-cadherin and SMA, we were able to label and distinguish urothelial cells and smooth muscle cells, respectively (Figure 8A-B). Control ureters have a discrete population of multilayered urothelial cells surrounded by a distinct smooth muscle layer. However, by E18.5, Sec10-CKOs experience near-total disappearance of all urothelial cells; almost all the cells forming the obstruction were smooth muscle actin positive.

There are two possible reasons for this noticeable decrease in urothelial cells in Sec10-CKOs: (1) the urothelial cells fail to develop, or (2) the urothelial cells develop but then are lost. To differentiate between these two scenarios, we used Rosa26-tdTomato Cre-reporter mice to track the fate of urothelial cells in the embryonic ureter. As previously described, whole mount imaging of the urinary tract demonstrated fluorescence only in cells derived from the UB.

We found that control and Sec10-CKO urothelia were similar in appearance and morphology at E16.5, indicating that initial urothelial development is intact (Figure 8C-D). However, by E17.5, there was a significant loss of the red-labeled urothelial cells in Sec10-CKO ureters with complete disappearance of these cells by E18.5 (Figure 8E-F). By demonstrating that ureteric bud derived urothelial cells do not contribute to the obstruction, these data eliminate epithelial-mesenchymal transition as a possible source of the mesenchymal cells that make up the obstruction formation.

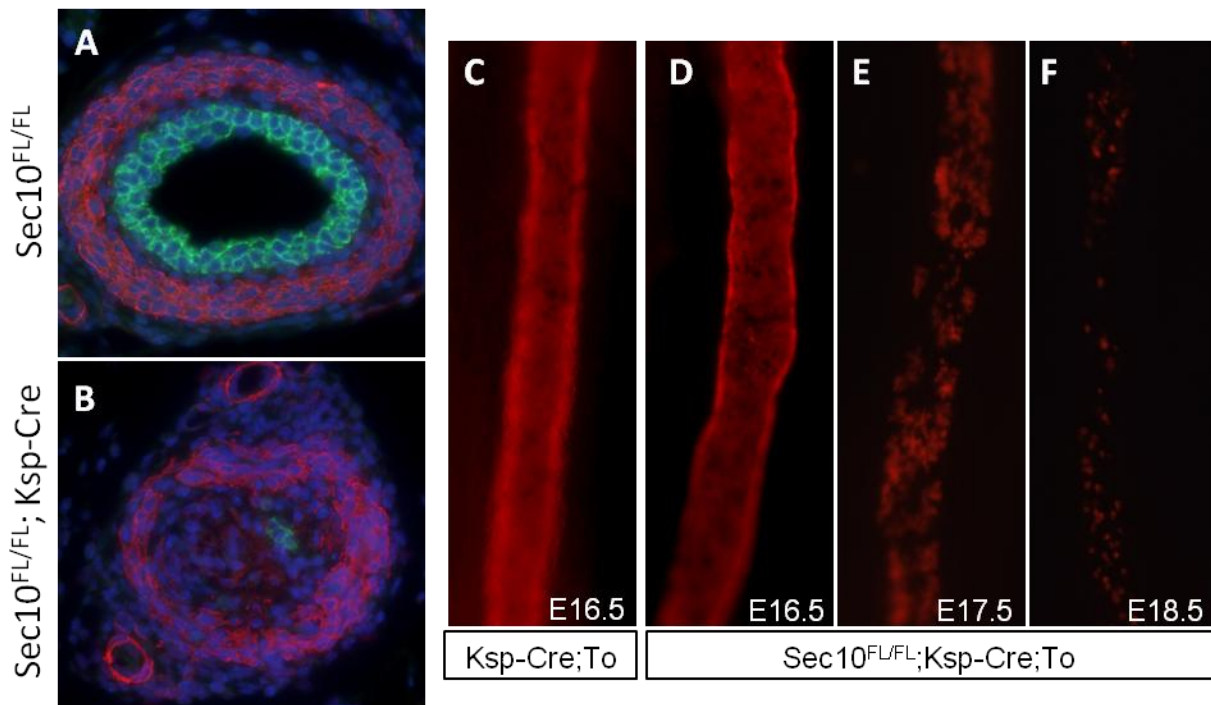


Figure 8. Ureter urothelial cells lacking Sec10 expression disappear during development and do not contribute to the cell population forming the UPJ obstruction

(A, B) Immunohistochemistry of newborn ureter sections labels the inner epithelial layer (E-cadherin; green) surrounded by a smooth muscle layer (SMA; red). Urothelial cells are almost completely lost in the UPJ of CKO mice. (C-F) Fluorescence microscopy of whole mount E16.5 *Ksp-Cre;To* control ureters, and of E16.5-E18.5 *Sec10^{FL/FL};Ksp-Cre;To* mutant ureters, showing progressive loss of tdTomato-labeled urothelial cells starting after E16.5.

Because the exocyst plays a role in trafficking vesicles to specific regions of the plasma membrane, we were interested to see if the exocyst plays a role in barrier function. We tested the integrity of the urothelial barrier by injecting FITC-dextran into the renal pelvis and allowed it to flow into the bladder. In control mice, the FITC-dextran flowed through the ureter into the bladder and there was no detectable FITC-dextran after sectioning, indicative of a strong luminal barrier (Figure 9A). However, Sec10-CKO mice showed a drastic increase of FITC dextran retained in the ureter, depicted by green fluorescence. Fluorescence is visible not just in the lumen of the ureter, as could be expected from impaired urine flow, but also in the deeper ureter tissues, including the smooth muscle layer. The penetration of FITC-dextran into these underlying tissues demonstrate increased permeability of the urothelial barrier (Figure 9B)

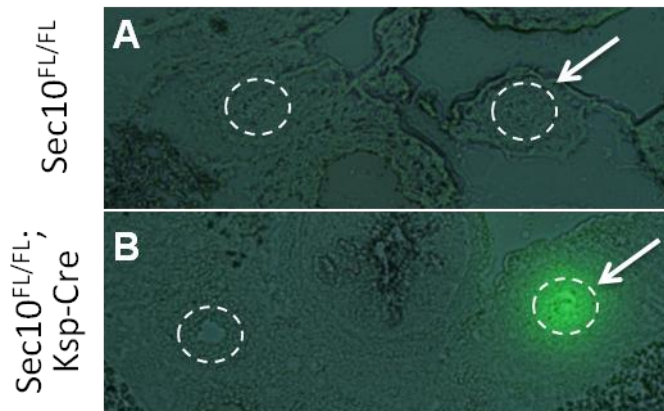


Figure 9. Sec10^{FL/FL};Ksp-Cre mice have a leaky urothelial barrier at E17.5

(A,B) FITC-dextran was injected into the left renal pelvis of E17.5 embryos. Images show cryosections of the ureters (circled; arrow denotes left ureter). Sec10^{FL/FL};Ksp-Cre mice (B) showed a drastic increase in dextran retention in the injected ureter tissue, indicating leakiness of the urothelial barrier. Images contributed by Brent Fujimoto.

Given that Sec10-CKO mice have a leaky urothelial barrier, we designed experiments to determine if the exocyst trafficked important barrier proteins to the correct location for proper function. There are two main categories of proteins that contribute to barrier function: (1) cell-cell adhesion proteins, and (2) hydrophobic plaques on the luminal surface of urothelia.

To investigate cell-cell adhesion, we used immunohistochemistry to stain for the tight junction marker, ZO-1 (Figure 10A-H). While there did not appear to be any significant differences at E16.5, there was a notable decrease in the number of tight junctions by E17.5 in Sec10-CKOs,

and almost complete loss by E18.5. It is important to consider that there is a significant disappearance of urothelial cells by E17.5. Thus, analysis of tight junction occurrence and frequency beyond this time point is problematic. Interestingly, the ZO-1 staining was in the correct localization and there were no detectable pockets of ZO-1 staining or diffuse staining throughout the cell. This indicates that the decreased ZO-1 staining is not due solely to decreased trafficking as there is also a decrease in ZO-1 protein levels.

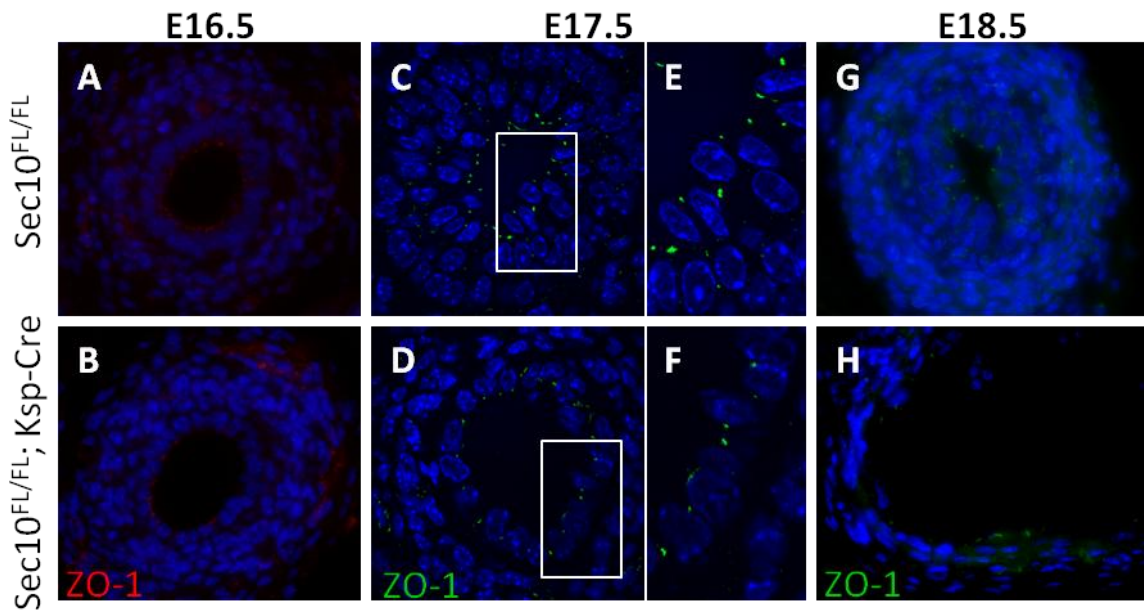


Figure 10. Sec10^{FL/FL};Ksp-Cre mice have decreased tight junctions in the urothelium at E17.5
 (A,B) Immunostaining at the UPJ region of E16.5 embryos confirmed a decrease in tight junctions, marked by ZO-1 (red). (C-F) Immunostaining at the UPJ region of E17.5 embryos for ZO-1 (green), imaged with a confocal microscope. (E, F) Images of boxed region of C and D are shown at increased magnification in E and F, respectively. (G, H) Immunostaining at the UPJ region of E18.5 embryos for ZO-1 (green). In all images, nuclei were counterstained with DAPI.

To investigate the second category of proteins that form the functional barrier, we immunostained for the four uroplakins that make up the luminal hydrophobic plaques; uroplakins are integral to the efficacy of the mature urothelial barrier against urine. We predicted uroplakins would be a strong candidate for exocyst trafficking because exocyst is known to traffic intracellular vesicles tagged with Rab8, Rab11 and Rab27, and uroplakin-containing vesicles have been also shown to carry these same protein tags. We immunostained embryonic ureters for each of the uroplakins: UPK1a, UPK1b, UPK2 and UPK3 (Figure 11A-H). At E17.5, CKO ureters

showed little to no detectable amounts of these uroplakins and, like ZO-1, there did not seem to be any ectopic expression of these proteins. If barrier function were impaired because the exocyst traffics uroplakins to the luminal surface in Sec10-CKO urothelial cells, we may expect to see diffuse staining throughout the cell, but not at the apical surface. Instead, we found that uroplakin proteins were not present in detectable amounts at E17.5. This raised the question: is the decrease in uroplakins due to a decrease in transcription or a decrease in protein stability?

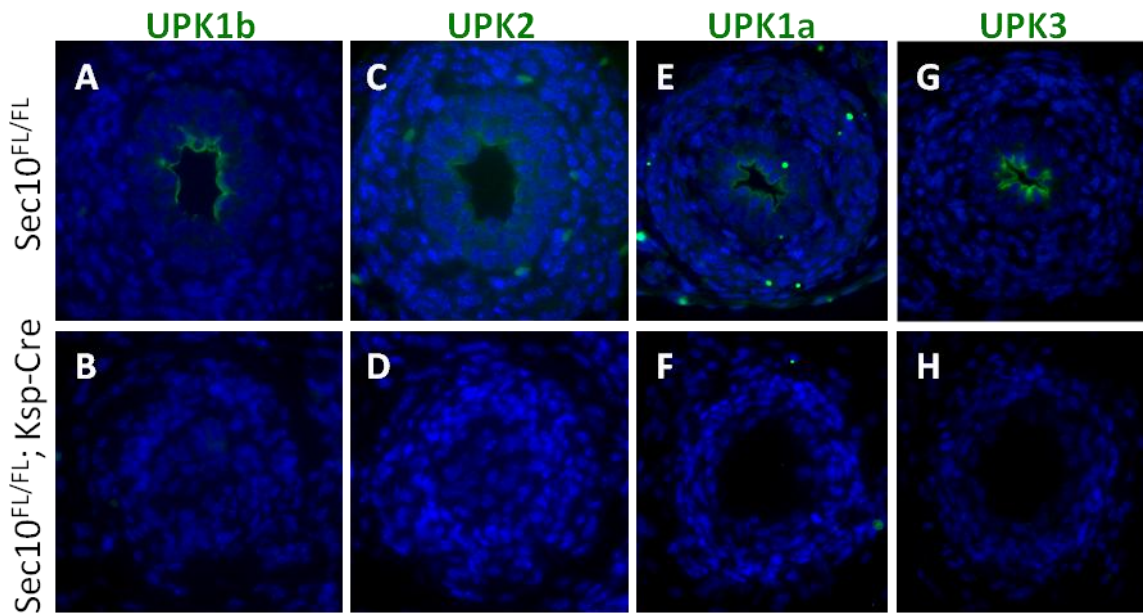


Figure 11. Sec10^{FL/FL};Ksp-Cre mice have no detectable uroplakins at E17.5

(A-H) Immunostaining at the UPJ region of E17.5 embryos; CKO mice showed decrease in apical localization of uroplakins (green), including UPK1a, UPK1b, UPK2, and UPK3. In all images, nuclei were counterstained with DAPI.

Sec10-CKO mouse ureters have impaired differentiation of urothelial cell layers

To address whether the decrease in uroplakins was due to decreased mRNA levels or decreased protein stability, we measured mRNA expression for each of the four uroplakins. We dissected mice of various embryonic ages and extracted RNA from the UPJ region (see Figure 7E for UPJ dissection diagram). Using reverse transcriptase, we were able to generate the cDNA complements to the extracted mRNA. Using real time quantitative PCR (qPCR) and primers for

genes of interest, selected from outside publications using qPCR on B6 mice, we analyzed the copy number of those cDNA templates to calculate the relative mRNA expression compared to the house-keeping gene β -actin. Calculations were made using the delta-delta Ct method (Fogelgren, et al. 2009), and normalized with control E15.5 expression set to 1 for each gene.

We measured mRNA levels utilizing two different approaches: (1) individual samples analyzed separately (Figure 12A-D), and (2) pooled samples of each genotype analyzed together (Figure 12E-H). These methods allowed us to compare results of biological replicates versus technical replicates for the mRNA analysis.

Using qPCR, expression of all four uroplakin genes were significantly decreased in CKO mice (Figure 12). We found that the general trends between our methods were very similar: control mice had an exponential increase in all uroplakin mRNA levels from E15.5 to E18.5, while Sec10-CKO ureters showed no increase in uroplakin mRNA and in most cases even decreased from E15.5 to E18.5. This suggests that E15.5-E18.5 is a critical time period for maturation of terminal superficial cells and for development of a strong urothelial barrier. The failure of Sec10-CKO ureters to express these genes at this point suggests a defect in superficial cell differentiation.

Note that the y-axes of these graphs are not to the same scale. Control E18.5 mice showed a 30.1 fold and 55.7 fold increase in UPK1a expression compared to E15.5, when analyzed as individual and pooled samples, respectively. Meanwhile, E18.5 CKO mice showed 738 fold and 888 fold increase in UPK1a expression compared to age-matched control mice, when analyzed as individual and pooled samples, respectively. Therefore, we conclude that values generated from both methods are representative of the trends in data. Individual E15.5 samples show much more variability than the pooled samples, and since the relative expression is based in E15.5 control mice, this can have significant effects on relative expression at later time points. This accounts for the discrepancies between the two methods, and indicates that pooled samples can be reliably used to report trends in the data.

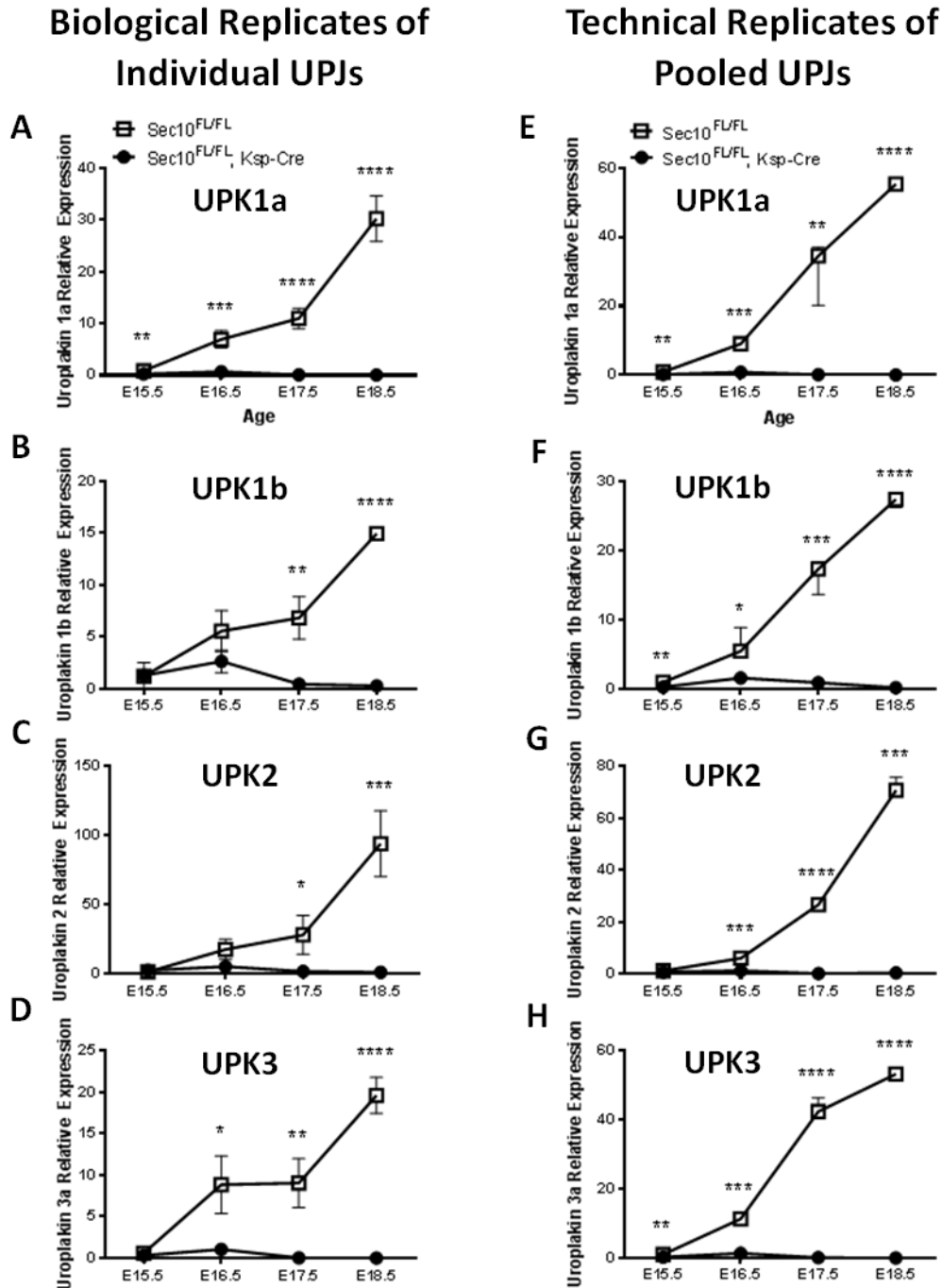


Figure 12. $Sec10^{FL/FL};Ksp-Cre$ ureters have decreased transcription of uroplakins

(A-D) Real time qPCR measurement of *Upk1a*, *Upk1b*, *Upk2*, and *Upk3a* gene expression in $Sec10^{FL/FL};Ksp-Cre$ and $Sec10^{FL/FL}$ UPJ regions of the ureter, collected from individual E15.5 - E18.5 embryo samples. Each data point represents the mRNA expression of multiple ureters of the same age and genotype measured individually with n=3 or n=4; however, the control E15.5 time point of *Upk2* has n=2. (E-H) Real time qPCR measurements of uroplakin expression collected from pooled UPJ ureter samples from ages E15.5-E18.5. Each data point represents the mRNA expression of three pooled ureters of the same age and genotype, relative to the expression in E15.5 control UPJs. (* p<0.05, ** p<0.01, *** p<0.001, **** p<0.0001). Ct values for each gene were normalized against beta actin.

In these UPJ samples, we also investigated the expression of PPAR γ , a transcription factor critical for terminal differentiation of urothelial cells. PPAR γ is not only an upstream regulator of uroplakin expression, but also a transcription factor for terminal urothelial differentiation, specifically of superficial cells (Weiss, et al. 2013). We found Sec10-CKO UPJs have significantly decreased PPAR γ mRNA expression starting at E16.5 (Figure 13). Together with the decrease in tight junctions and absence of uroplakin gene expression, this provides strong evidence that the Sec10-CKO urothelium fails to differentiate.

We know that there is a progressive loss of urothelial cells at E17.5 in Sec10-CKO ureters, and because urothelial cells produce PPAR γ , it would make sense to see less PPAR γ expression at this time point. However, the decline in PPAR γ starts by E16.5, preceding the loss of urothelial cells (Figure 13A-B).

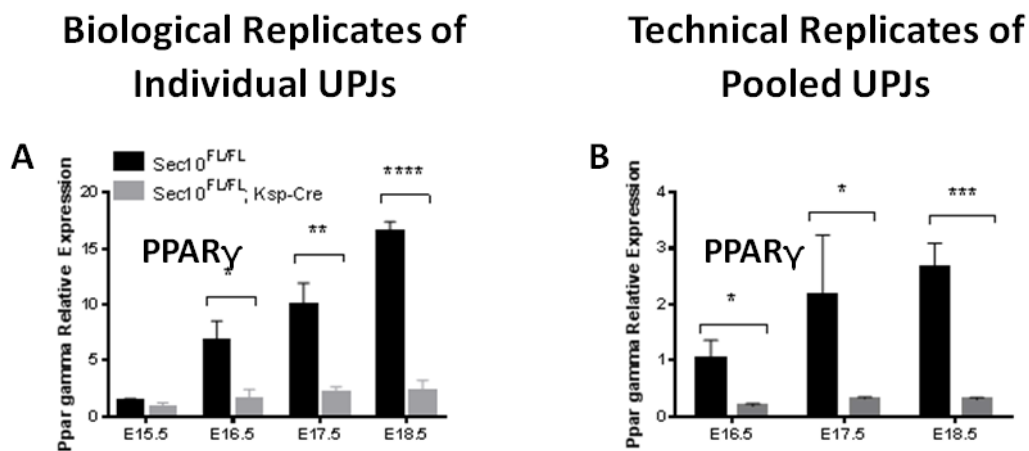


Figure 13. Sec10^{FL/FL};Ksp-Cre ureter urothelial cells fail to differentiate

(A) Real time qPCR measurement of *PPAR γ* gene expression in *Sec10^{FL/FL};Ksp-Cre* and *Sec10^{FL/FL}* UPJ ureters collected from E15.5 - E18.5 embryos. Each data point represents the mRNA expression of multiple ureters of the same age and genotype measured individually with n=3 or n=4. (B) Real time qPCR measurement of *PPAR γ* gene expression in *Sec10^{FL/FL};Ksp-Cre* and *Sec10^{FL/FL}* UPJ ureters collected from E15.5 - E18.5 embryos. Each data point represents the mRNA expression of three pooled ureters of the same age and genotype (* p<0.05, ** p<0.01, *** p<0.001, ****p<0.0001). Ct values for each gene were normalized against beta actin.

Sec10-CKO UPJs significantly decreased PPAR γ expression. This key finding is the earliest abnormality, mechanistically, that we have been able to detect in Sec10-CKOs. PPAR γ is significantly decreased at E16.5, an entire day before morphological differences are visible in

histology. It provides evidence that exocyst function is required for normal differentiation. It is possible that all successive steps leading up to UPJ obstruction are based on this failure of differentiation; however, it cannot be ruled out that impaired exocyst function is required for the subsequent steps resulting in obstruction.

Having established that urothelial differentiation is impaired in Sec10-CKOs, we were interested to know if there was also an effect on the development of progenitors. To study the progenitor population over time, we used immunostaining of UPJ regions to mark urothelial progenitor cells. We stained for p63, which is required for proliferative self renewals of the progenitor population (Bultman, et al. 2000). P63 is a marker for basal and intermediate cells (Gandhi, et al. 2013), as seen in control E18.5 ureters (Figure 14).

At E16.5, the urothelium is comprised of a monolayer of cells in both control and Sec10-CKO mice (Figure 14A-B). At E17.5, the control urothelium begins to stratify, while the Sec10-CKO urothelium fails to stratify. Between E16.5 and E17.5, Sec10-CKO urothelium experiences a significant loss in p63 positive cells (Figure 14C-D). This would suggest that some of the p63 positive cells in E16.5 embryos will disappear by E17.5, possibly from cell death or from detaching from the basement membrane. By E18.5, Sec10-CKO UPJs have no surviving urothelial progenitors.

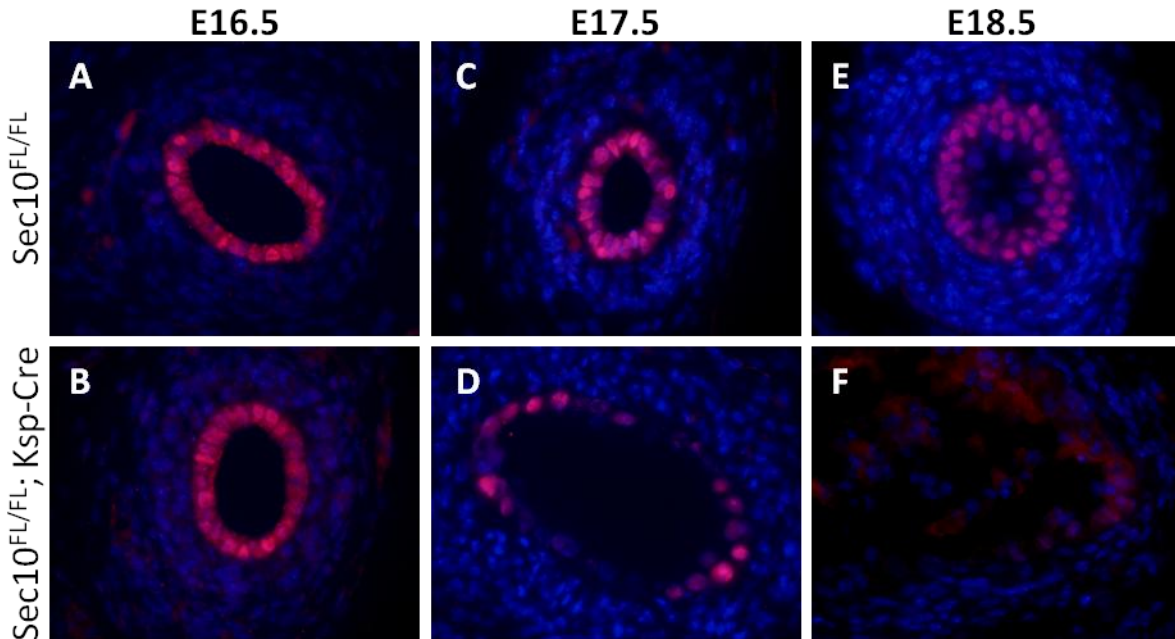


Figure 14. $Sec10^{FL/FL};Ksp-Cre$ urothelial basal and intermediate cells begin to disappear at E17.5
 (A-E) Immunohistochemistry of urothelial progenitor marker, p63 (red), in E16.5-E18.5 $Sec10^{FL/FL};Ksp-Cre$ and $Sec10^{FL/FL}$ ureters showed no detectable differences at E16.5. There was progressive loss of p63 positive cells, consistent with the concurrent loss of the urothelial layer. In all images, nuclei were counterstained with DAPI.

Sec10-CKO mouse ureters undergo a fibrotic wound-healing starting at E17.5

To determine which cell type is over proliferating to contribute to obstruction formation, we immunostained for both smooth muscle actin and Ki67, a marker for cell proliferation (Figure 15A-B). Quantification analyses of immune-stained cross sections show increased proliferation rates of smooth muscle actin positive cells in E17.5 Sec10-CKO ureters, compared to control littermates (Figure 15C).

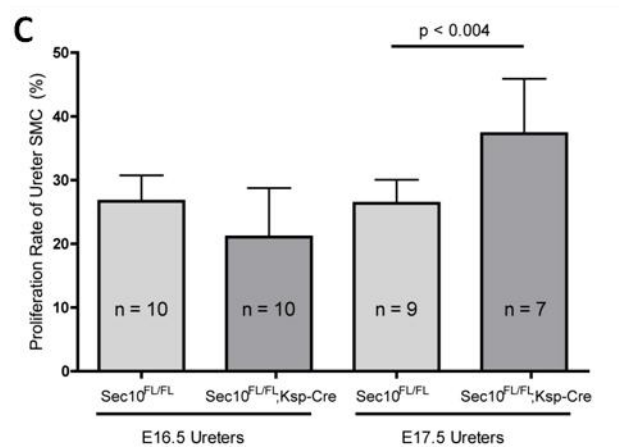
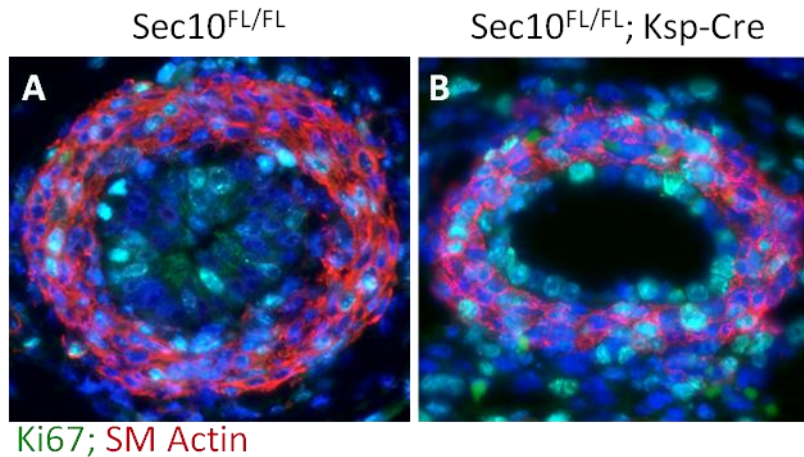


Figure 15. Sec10^{FL/FL};Ksp-Cre mice develop an obstruction in the ureteropelvic junction (UPJ) by E18.5. from over-proliferation of SMA⁺ cells

(A,B) Immunohistochemistry of E17.5 ureter sections labels proliferating cells (Ki67; green) and SMA positive cells (red). Nuclei were counterstained with DAPI. (C) Proliferation rates were calculated from counting all Ki67⁺;SMA⁺ cells and Ki67⁻;SMA⁺ cells in Sec10^{FL/FL};Ksp-Cre and control ureters at E16.5 and E17.5. Proliferation rates were compared between mutant and control ureters by student t-tests, with means \pm SD and n's (n=ureters) for each group shown. Quantification analysis contributed by Noemi Polgar.

However, smooth muscle actin can be used to mark either smooth muscle cells or myofibroblasts. Fibroblasts are cells found in all tissues, and are involved in extracellular matrix production. Fibroblasts can differentiate into myofibroblasts in response to tissue injury; myofibroblasts migrate to the wound and release cytokines to regulate the repair process (Baum and Duffy 2011) and have also been implicated in fibrotic processes (Eyden 2008). Therefore, we hypothesized that the smooth muscle actin positive cells obstructing the lumen of the UPJ are myofibroblasts and not smooth muscle cells.

To test this, we measured mRNA levels for two proteins that suggest a myofibroblast phenotype. Unfortunately, there is no one definitive marker for myofibroblasts; therefore it is crucial to investigate the expression of several genes indicative of myofibroblasts. We measured expression of fibroblast specific protein 1 (S100A4), which was found to be elevated in Sec10-CKO UPJs starting at E17.5 (Figure 16B,E). We also measured mRNA levels for periostin, a matricellular protein shown to promote myofibroblast differentiation (Elliott, et al. 2012) and myofibroblast persistence (Crawford, et al. 2015). We found a weak trend for increased periostin expression in Sec10-CKOs that reached statistical significant in analyses of pooled E16.5 UPJ samples (Figure 16A,D).

We also wanted to measure expression of genes specific to smooth muscle cells. We chose desmin, an intermediate filament protein, as an indicator for smooth muscle cells. While it has been shown that some lesional fibroblasts express desmin, myofibroblasts in normally healing granular tissue do not express desmin (Skalli, et al. 1989). In fact, it has been well accepted that negative staining for desmin is a stronger indicator for the myofibroblast cell type; positive staining for desmin can be more ambiguous, but is generally favored as an indicator for the smooth muscle cells (Eyden 2008). We used real time qPCR to measure desmin mRNA expression in our collected UPJ samples and found no significant differences in desmin expression between control and Sec10-CKO UPJs at any time point when analyzed individually (Figure 16C), but a statistically significant decrease in expression when analyzing pooled samples (Figure 16F). It makes sense that there might not be drastic changes in desmin expression because we measured the mRNA in the entire UPJ region, including the smooth muscle layer. In essence, these findings show there is no increase in the number of smooth muscle cells in Sec10-CKOs compared to control mice.

Together, these findings support our hypothesis that myofibroblasts contribute to the cell population that obstructs the UPJ in Sec10-CKO mice, not smooth muscle cells. We have already ruled out EMT, due to the loss of Tomato positive cells at the obstruction, indicating the urothelial lineage does not contribute to the obstructing cell population. Therefore, the myofibroblasts must migrate into the lumen, likely signaled by an insult to the urothelium. The

loss of urothelial cells starts at E17.5, and the increased expression of myofibroblast markers shortly follow, suggesting a possible injury at or before E17.5.

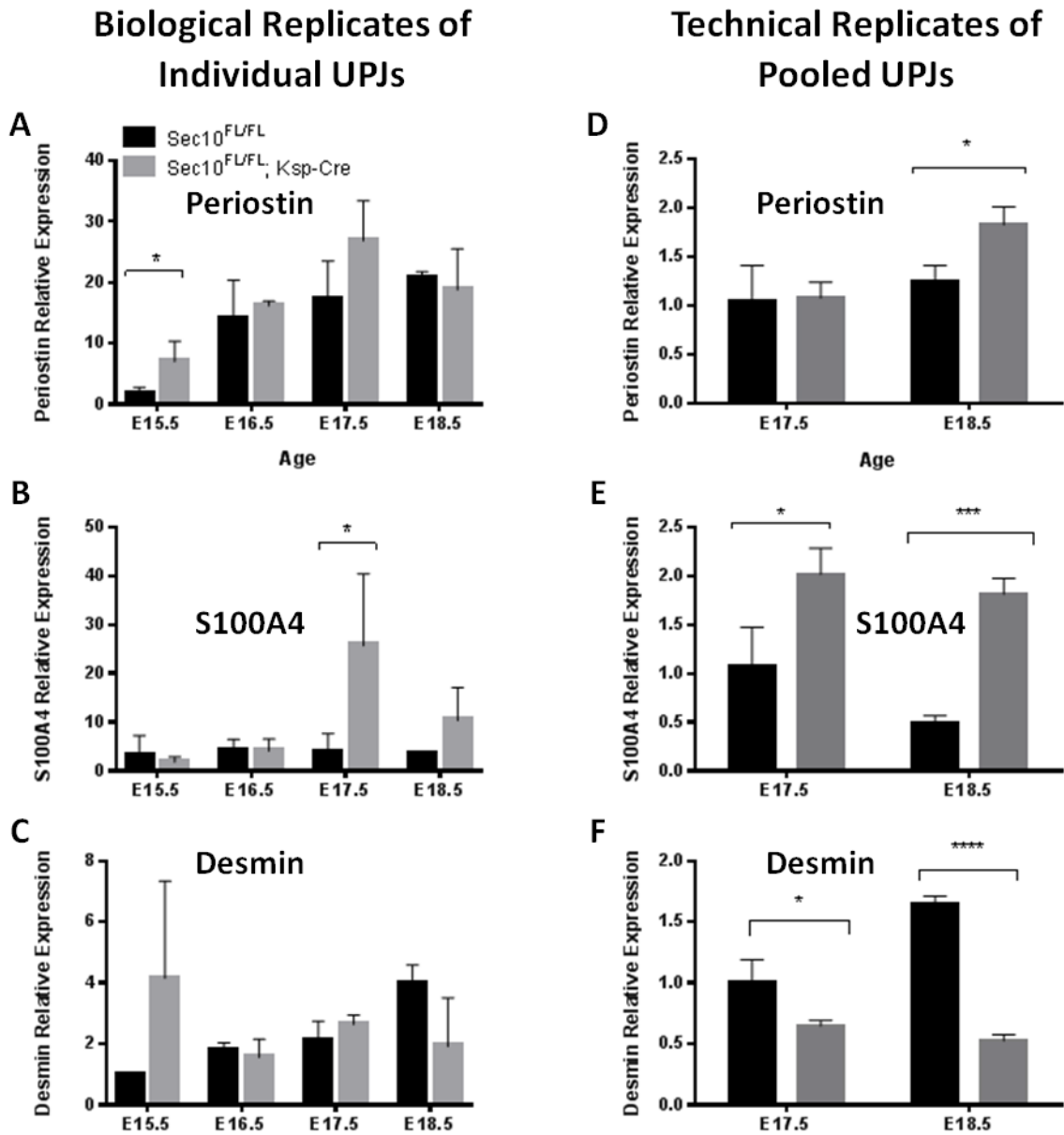


Figure 16. $Sec10^{FL/FL};Ksp-Cre$ UPJ ureter obstructions are likely due to myofibroblast activation

(A-C) Real time qPCR measurement of gene expression of fibroblast marker *S100A4* and myofibroblast marker periostin and smooth muscle marker desmin, in $Sec10^{FL/FL};Ksp-Cre$ and $Sec10^{FL/FL}$ UPJ regions of the ureter, collected from individual E15.5 - E18.5 embryo samples. Each data point represents the mRNA expression of multiple ureters of the same age and genotype measured individually with n=3 or n=4. (D-F) Real time qPCR measurements of gene expression of the same markers, collected from pooled UPJ ureter samples from ages E17.5-E18.5. Each data point represents the mRNA expression of three pooled ureters of the same age and genotype. (* p<0.05, ** p<0.01, *** p<0.001, ****p<0.0001). Ct values for each gene were normalized against beta actin.

Sec10-CKO UPJs have significantly increased TGFβ1 expression. We found evidence of myofibroblast activation, a hallmark of both wound healing and fibroproliferation. Using real time qPCR, we also measured the mRNA levels of TGFβ1, a critical regulator of myofibroblast activation and other processes in fibrotic wound healing, including increased extracellular matrix deposition. Sec10-CKO UPJs experienced a 2.4 (Figure 17A) to 3.4 (Figure 17B) fold increase in TGFβ1 expression starting at E17.5, depending on sample preparation method. This key finding provides evidence supporting a fibrotic wound healing response as the signaling lynch pin on which this type of congenital obstruction develops, and opens a realm of possible therapeutic drug targets.

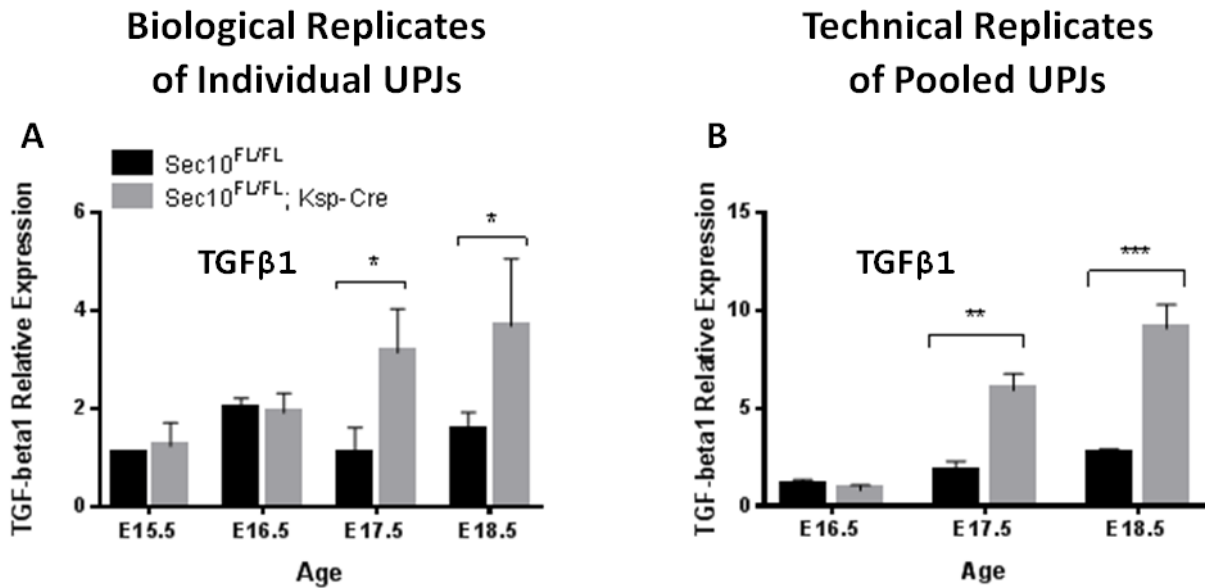


Figure 17. Sec10^{FL/FL};Ksp-Cre UPJs have increased TGFβ1 expression at E17.5.

(A) Real time qPCR measurement of gene expression of fibrotic wound healing marker *TGFβ1* in *Sec10^{FL/FL};Ksp-Cre* and *Sec10^{FL/FL}* UPJ regions of the ureter, collected from individual E15.5 - E18.5 embryo samples. Each data point represents the mRNA expression of multiple ureters of the same age and genotype measured individually with n=3 or n=4; however, the control at E15.5 has only n=2. (B) Real time qPCR measurements of gene expression of *TGFβ1*, collected from pooled UPJ ureter samples from ages E16.5-E18.5. Each data point represents the mRNA expression of three pooled ureters of the same age and genotype. (* p<0.05, ** p<0.01, *** p<0.001, ****p<0.0001). Ct values for each gene were normalized against beta actin.

The disappearance of urothelium, the increase in proliferation of SMA-positive cells, the increase in fibroblast markers, and the increase in TGF β 1 expression all start at E17.5. This coincides with the time urine production initiates, around E16.5. This timing provides the basis of our working hypothesis: a leaky urothelial barrier allows some urine to permeate into and damage the underlying tissues, initiating a fibrotic wound-healing response. This possibility is supported by our explant experiments, where Sec10-CKO ureters that are dissected and grown in culture, do not form an obstruction in the absence of urine, but still lose urothelial cells (data not shown).

Another hallmark of fibroproliferation is dysregulation of extracellular matrix deposition, including collagens. Collagen IV makes up the scaffold on which the basement membrane is formed (Paulsson 1992), so we were able to visualize the basement membrane with immunostaining for collagen IV. The basement membrane is an extracellular matrix structure that separates epithelial cells from other tissue compartments, and further is able to regulate cell behavior (Paulsson 1992). In control ureters, the basement membrane formed a discrete border between the urothelial layer and the smooth muscle layer (Figure 18A). However, Sec10-CKO ureters have severely disorganized basement membranes (Figure 18B).

The clear difference in the collagen IV deposition pattern is likely caused by stromal remodeling, a process which involves matrix degradation using enzymes like matrix metalloproteinases (MMPs), followed by new deposition of matrix. It is likely that this remodeling will also affect how the basement membrane influences the local cell populations. Further, it would be interesting to investigate when the basement membrane is first disrupted, as (1) a leaky basement membrane may allow urine to have increased permeability to deeper tissues, and (2) urothelial cells attached to a portion of the basement membrane that is digested may detach or undergo cell death.

This remodeling was accompanied with increased collagen IV mRNA expression at E18.5 (Figure 18C). We also investigated expression of another component of the extracellular matrix fibronectin (FN). Specifically, we measured expression of the FN splice variant associated with myofibroblast activation: ED-A (Serini, et al. 1998). Here we measured significant increase in ED-A FN expression in E17.5 Sec10-CKOs (Figure 18D), providing further support for our

hypothesis of a fibroproliferative wound healing event contributing to UPJ obstruction formation in these mutant ureters.

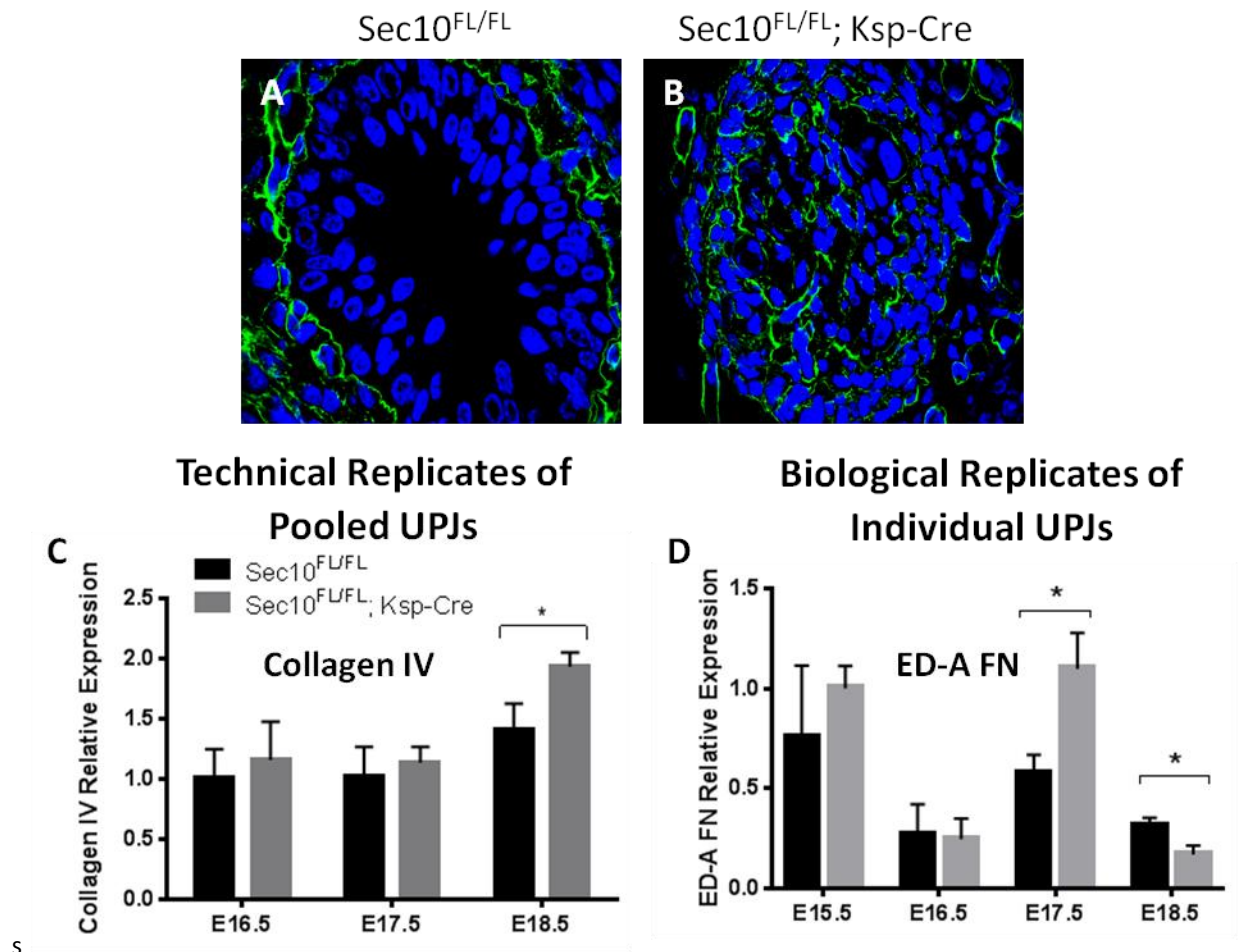


Figure 18. Sec10^{FL/FL};Ksp-Cre UPJ ureter obstructions have dysregulation of ECM deposition and basement membrane organization

(A,B) Immunohistochemistry of E18.5 ureter sections labels basement membrane by staining Collagen IV (green); *Sec10^{FL/FL};Ksp-Cre* ureters show remodeling of the basement membrane. (C) Real time qPCR measurements of gene expression of Collagen IV, collected from pooled UPJ ureter samples from ages E16.5-E18.5. Each data point represents the mRNA expression of three pooled ureters of the same age and genotype. (D) Real time qPCR measurements of gene expression of fibronectin splice variant ED-A, collected from individual UPJ ureter samples from ages E15.5-E18.5. Each data point represents the mRNA expression of multiple ureters of the same age and genotype measured individually with n=3 or n=4. (* p<0.05). Ct values for each gene were normalized against beta actin.

Discussion

Summary of Findings

We found that Sec10-CKO mice experience impaired urothelial differentiation in the ureter; this is first detectable by decreased mRNA levels of a key regulator of urothelial differentiation, PPAR γ , at E16.5. By E17.5, the Sec10-CKO urothelial barrier is leaky. In this same time period, a luminal fibrotic wound healing response initiates, activating myofibroblasts to overproliferate and obstruct the lumen of ureter at the UPJ region.

Why is the UPJ a Hotspot for Obstructions?

Sec10-CKO mice develop bilateral obstructions at the ureteropelvic junction (UPJ), the most common site for congenital obstructions in humans that cause prenatal hydronephrosis. Why is this specific site so vulnerable to obstruction? This region forms from three different cell lineages: (1) the ureteric bud, (2) the nephrogenic mesenchyme of the intermediate mesoderm, and (3) the tail-bud mesoderm (Brenner-Anantharam, et al. 2007). The complexity of these interactions and cell integration may explain the sensitivity of this region: disturbances can affect the peristaltic machinery; developmental delays can result in undifferentiated urothelial cells being exposed to urine. This region develops its functional barrier from urine very shortly before urine exposure, making it crucial that the signaling events required for said development are completed. Control UPJs do not stratify until E16.5, which leaves a narrow window for development before the start of urine flow. This co-development does not appear to have many redundancies or compensatory systems in place to prevent urine exposure, should the barrier be incomplete. In fact, UPJ urothelium seems to stratify almost concurrently with the start of urine production: E16.5. If normal UPJ formation is delayed even slightly, this would leave UPJ cells vulnerable to damage from urine exposure.

Another potential contributor is that the renal pelvis is larger in circumference than the ureter. As the first portion of the ureter, the UPJ must accommodate the larger volume of urine held in the renal pelvis and facilitate its passage. The UPJ represents a “bottleneck” of the collecting

system, and may be exposed to increased hydrostatic pressure and exacerbates the stretch-potential of the luminal surface, increasing leakiness of the urothelial barrier.

Consequence of Urine Exposure to Interstitial Tissues of the Ureter

Protein localization of uroplakins and ZO-1, a protein found in tight junctions, indicated that urothelial cells failed to form a normal functional barrier. Other studies have found that urothelia has impaired barrier function when missing uroplakins (Hu, et al. 2002) or tight junctions (Smith, et al. 2015).

Urine contains toxic factors that injure urothelium (Parsons, et al. 2000). Given that Sec10-CKO mice have a permeable urothelial barrier, urothelial cells and the underlying mesenchyme will be exposed to urine when urine production initiates, around E16.5 (Bohnenpoll and Kispert 2014).

Some of the toxic factors in urine further increase the permeability of the urothelia it injures (Rajasekaran, Stein, and Parsons 2006). There are urinary proteins that protect urothelia from these toxic factors, including heparin and Tamm-Horsfall protein (Parsons, et al. 2000). In fact, interstitial cystitis is a painful condition caused by increased permeability of bladder urothelium; similar to the increased permeability of ureter urothelium in our Sec10-CKO. Individuals with interstitial cystitis tend can have defective mutations of the Tamm-Horsfall protein (Parsons, et al. 2007).

The Sec10-CKO mouse model may be a means of studying how increased barrier permeability contributes to the development of a UPJ obstruction. We may also be able to knock out Sec10 in the adult bladder to test if this creates a novel mouse model of interstitial cystitis. In human cases, this increased urothelial permeability may have other causes, like defective Tamm-Horsfall protein.

Intraluminal Wound Healing as an Underlying Mechanism of Obstruction

We measured a significant increase in TGF β 1 expression in Sec10-CKO ureters at E17.5 and after, which at least one study also found in human UPJ obstructions (Yang, et al. 2006). TGF β 1

is known to play several roles in tissue fibrosis, including fibroblast activation and ECM accumulation. The TGF β superfamily members bind to a Type I and a Type II transmembrane kinase receptor to transduce intracellular signaling.

Renal fibrosis models with TGF β 1 mediated effects have been shown to use Type I receptor ALK5 to induce kidney fibrosis. ALK5 phosphorylates Smad2 and Smad3, thereby activating them. Once activated, Smad2 and Smad3 form a heteromeric complex with Smad4 and subsequently are transported to the nucleus. This Smad complex binds to specific DNA regions to modify gene expression (Massague and Wotton 2000). Some of the target genes include collagens, fibronectin, connective tissue growth factor (CTGF), and TIMP-1 (Munoz-Felix, et al. 2015). TGF β 1 also increases expression of itself and of its Type II receptor (Diez-Marques, et al. 2002).

I was unsuccessful in optimizing a protocol to detect Smad signaling using either Western Blots or using immunohistochemistry. Therefore, we cannot yet conclude if the Smad signaling pathway is responsible for the TGF β -induced fibrosis. There are other known non-canonical TGF β signaling pathways that contribute to fibrosis including PI3k, MAPK, and Jun Kinase (Munoz-Felix, et al. 2015). Kidney fibrosis models have been shown to be mediated by ALK5-dependent Smad2 and Smad3 phosphorylation. But Smad2 and Smad3 seem to have opposing effects: Smad2 decreases fibrosis after UUO (Meng, et al. 2010), while Smad3 promotes fibrosis after UUO (Sato, et al. 2003). These opposing roles for Smad2 and Smad3 have also been found in peritoneal fibrosis (Duan, et al. 2014) and hepatic fibrosis (Zhang, et al. 2015).

There are also Smads, including Smad6 and Smad7, that antagonize Smad2 and Smad3's pro-fibrotic role by competing for binding to the Smad4 co-receptor or by binding the Type I receptor (Derynck and Zhang 2003). Given the complexity of TGF β signaling, further experiments are necessary to determine the pathway involved in TGF β -mediated fibrosis in SEC10-CKO ureters so that antagonists for those pathways can be tested to rescue the phenotype. These findings could open the door for potential drug targets.

It is interesting to note that PPAR γ decreases TGF β 1 expression and activation, including Smad-dependent and Smad-independent pathways (Wei, et al. 2012). Therefore, it is possible that

loss of PPAR γ not only impairs superficial cell differentiation, but also allows for TGF β 1 dysregulation, and therefore *fibrotic* wound healing. PPAR γ agonists may be able to induce apical uroplakin expression and reduce TGF β - mediated fibrosis so as to delay the formation of or minimize the size of the UPJ obstruction. This is supported by the fact that reduced PPAR γ expression is associated with fibrosis and that treatment with PPAR γ ligands ameliorated kidney fibrosis (Zheng, et al. 2002).

This is an exciting possibility because there are already FDA approved agonists available on the market, including: Thiazolidinediones (TZDs) or synthetic ligands of PPAR γ widely used in the clinical setting. TZDs attenuated renal interstitial fibrosis and inflammation in the UUO model of tubulo-interstitial fibrosis (Kawai, et al. 2009). TGF β 1 also induces expression of ED-A, the splice variant of fibronectin during wound healing and fibrosis (Leask and Abraham 2004). ED-A FN deposition precedes SMA expression by fibroblasts after TGF β stimulation and also during granulation tissue formation (Serini, et al. 1998).

ED-A FN is upregulated following injury of peripheral nerves (Mathews and French-Constant 1995), is essential for proper wound repair of skin (Muro, et al. 2003), is critical for cell migration (Inoue, et al. 2001), is essential for myofibroblast activation, and has been shown to be activated by TGF β 1 (Muro, et al. 2008). Consistent with this, Sec10-CKO UPJs show increased mRNA expression of both TGF β 1 and ED-A FN at E17.5. Both of these genes are associated with myofibroblast activation. Fibroblast specific protein 1 (S100A4) and periostin show significant increases in mRNA expression at E17.5 and E18.5, respectively. This gene expression profile suggests myofibroblast activation, at or immediately following ED-A FN and TGF β 1 upregulation.

To address the statistically significant increase in periostin mRNA in Sec10-CKOs at E15.5, we do not believe that this is indicative of myofibroblast activation because the obstruction only starts to form two days later. Also, myofibroblasts migrate to sites of injury, but there are no apparent morphological changes that could indicate injury until E17.5, when there is disappearance of the urothelial layer. Therefore, this finding may be due to chance or may be due to the increased variability found in all qPCR analyses on E15.5 samples. Collection of the UPJ region is very difficult, especially at earlier time points; inclusion of any portion of the renal

pelvis or the lower ureter may change expression outcomes. Further, there is no change in S100A4 at this time point. Therefore, while this finding is interesting and merits consideration in future experiments, there simply is not enough data at this time to draw any strong conclusions.

Once synthesized, TGF β is secreted into the extracellular space in an inactive form: bound to latency-associated protein (LAP) and latent TGF- β -binding protein (LTBP). Release of LAP is required for TGF β binding to its receptors.

One possibility is that urinary damage in the Sec10-CKO ureter creates reactive oxygen species (ROS). Oxidation activates latent TGF β 1 by releasing LAP and can upregulate TGF β gene expression (Liu and Desai 2015). Not only does ROS induce TGF β 1 expression, TGF β 1 induces ROS (Liu and Desai 2015). Several pathways are involved in the TGF β -mediated induction of Nox4, an important ROS producer. Noxs are a group of heme-containing transmembrane proteins expressed by epithelial cells (Liu and Desai 2015). Independent of Smad, TGF β 1 induces Nox4 in kidney myofibroblasts (Bondi, et al. 2010). TGF β induces mitochondrial ROS that leads to expression of profibrotic proteins; this affect is attenuated by antioxidants, therefore, mitochondrial ROS is a potential target for treating excessive fibrosis (Jain, et al. 2013). Unfortunately TGF β 1 suppresses antioxidant enzymes including Superoxide dismutases (SODs), catalase, Grx (Liu and Desai 2015). Human tissue samples, animal studies, and in vitro studies of obstructive nephropathy have been found to have high expression of oxidative stress genes, Nos2 and Nos3, and decreased expression of antioxidants, SOD1 and Catalyse (Klein, et al. 2011). Studies have reported increased expression of nitric oxide synthetases Nos2 and Nos3 in human UPJ obstruction (Valles, et al. 2003).

In conclusion, the significant increase in TGF β 1 expression is a clear indication that the Sec10-CKO mouse is undergoing fibrotic wound healing following the onset of urine production (ie. after E16.5). The mechanism of fibrosis in this mouse is not entirely clear: (a) perhaps cells exposed to urine have increased oxidative stress that causes an upregulation of TGF β 1, (b) perhaps canonical Smad-mediated signaling may be responsible for the mesenchymal overproliferation, etc. Understanding this mechanism will help determine targets for future

drug treatment options. For example, recommending pregnant mothers to increase their intake of antioxidants may be a simple way to decrease risk of UPJ obstruction development.

Comparison of the Sec10-CKO to other Mouse Models

Our data shows that exocyst function is required for normal urothelial differentiation in the embryonic ureter. This loss of exocyst function results in an impaired functional barrier, which allows urine to permeate and damage ureter cells, resulting in a fibrotic wound healing response. In essence, loss of exocyst function increases susceptibility to urine damage, which contributes to the obstruction of the UPJ region. However, there are other mouse models that also have impaired functional barriers but do not result in this same phenotype.

Surgical models have studied the effects of ligating a ureter of a wildtype mouse, forming a unilateral ureter obstruction (UUO). This model is well studied as it provides the possibility to study the resultant kidney damage and physiological responses to ureter obstruction. However, this model cannot be used to investigate the *causes* of obstruction. A further limitation to this type of model is that these surgeries cannot be performed on developing embryos, and most cases of human UPJ obstructions are initially detected during pregnancy. Therefore, I will focus on genetic mouse models as they are uniquely suited to study disease development.

These knockout (KO) mouse models (summarized in Table 3 and Table 4) will be discussed in comparison to the Sec10-CKO model in order to better understand the mechanisms underlying UPJ obstruction formation.

Table 3. Summary of knockout mouse models for congenital ureter obstruction

Gene	Cause of hydronephrosis	Age	Urothelial abnormalities	Smooth Muscle abnormalities	Elevated gene/protein expression	Decreased gene/protein expression	Unchanged gene/protein expression	References
Cldn4	Urothelial thickening	~12 months	<ul style="list-style-type: none"> • Thick urothelium • Normal number and localization of TJs and UPKs. 	none reported	-	-	<ul style="list-style-type: none"> • Other claudins (altered localization). • UPKs. 	(Fujita et al., 2012)
UPK2	Urothelial thickening (and vesicoureter reflux)	70-80% penetrance at 4 months	<ul style="list-style-type: none"> • Hyperplastic. • Small S cells. • No UPK plaques 	none reported	<ul style="list-style-type: none"> • UPK1a mRNA • UPK1b mRNA • UPK3 mRNA 	<ul style="list-style-type: none"> • UPK1a, UPK1b, and UPK3 protein (abnormal localization) 	-	(Kong et al., 2004)
UPK3	Urothelial thickening (and vesicoureter reflux)	>50% penetrance at 2-3 weeks after birth.	<ul style="list-style-type: none"> • Hyperplastic. • Small S cells that frequently detach. • Lacks mature fusiform vesicles. • Small UPK plaques • Normal number of tight junctions. • Increased desmosomes. 	none reported	<ul style="list-style-type: none"> • UPK1a mRNA • UPK1b mRNA • UPK2 mRNA 	<ul style="list-style-type: none"> • UPK1a, UPK2 protein (normal localization) • UPK1b protein (abnormal localization) 	-	(Hu et al., 2000) and (Hu et al., 2002)

*Note: Each mouse model is a global knock out, and each results in a *physical* obstruction of the ureter.

**Descriptions of urothelium and smooth muscle are specific to the ureter.

Table 4. Summary of other knockout mouse models for genes of interest

Gene	Knockout	Cause of hydronephrosis	Age	Urothelial abnormalities	Smooth Muscle abnormalities	Decreased gene/protein expression	Unchanged gene/protein expression	Reference
PPARγ	Hoxb7-Cre: UB derived structures	not reported	Adult; 7.7% penetrance	<ul style="list-style-type: none"> Increased number of p63+ cells. Apical cells express basal cell markers (Krt5, Shh) 	none reported	Shh	Brg1, Δ Np63	(Weiss <i>et al.</i> , 2013)
ΔNp63	global	<i>no hydronephrosis</i>	N/A	<ul style="list-style-type: none"> Monolayer Decreased proliferation. 	none reported	-	Brg1, Shh, PPAR γ , UPKs	(Weiss <i>et al.</i> , 2013)
Brg1	Hoxb7-Cre: UB derived structures	Functional: diminished SM layer	E16.5; full penetrance by 3 weeks post birth	<ul style="list-style-type: none"> Monolayer 	<ul style="list-style-type: none"> Diminished SM layer 	UPKs, Cytok20, PPAR γ , p63, Shh, Tshz3, Myocardin	-	(Weiss, et al. 2013)
Tbx18	Global	Functional and Obstructive: Diminished SM layer. Partial structural ureter obstruction.	E18.5; full penetrance	<ul style="list-style-type: none"> Monolayer. Decreased proliferation at E15.5. 	<ul style="list-style-type: none"> Thin SMC layer Decreased proliferation Dislocalized to kidney. Fibrous. 	UPKs	-	(Airik, et al. 2006)
Shh	Hoxb7-Cre: UB derived structures	Functional: diminished SM layer	adult (congenital hydroureter)	none reported	<ul style="list-style-type: none"> Thin SMC layer Delayed differentiation Decreased proliferation 	-	-	(Yu, Carroll, and McMahon 2002)

**Descriptions of urothelium and smooth muscle are specific to the ureter.

Uroplakin Knockout Mouse Model

As discussed previously, uroplakins are required for intact functional barrier of the urothelium (Hu, et al. 2002). Both UPK2 and UPK3 knockout (KO) mice have been previously generated (Kong, et al. 2004; Hu, et al. 2000). They indeed have impaired urothelial barrier function and UPK3 KO ureters show that apical cells will peel off (Hu, et al. 2000), similar to what we see in Sec10-CKOs. By four months of age, some of the UPK KO mice develop hydronephrosis, caused at least in part by partial or complete ureter obstructions (Kong, et al. 2004). However, this obstruction is caused by the overgrowth of urothelium; whereas our Sec10-CKO ureters experience *in utero* urothelial degeneration and mesenchymal overgrowth.

This difference can possibly be attributed to the fact that UPK ablation will have less barrier permeability compared to UPK loss accompanied with decreased TJs. Further, UPK3 KO mice have increased desmosomes than control mice (Hu et al., 2000; Hu et al., 2002) potentially as a compensatory mechanism to limit barrier failure. Perhaps minimal penetrance of urine results in the proliferation of the superficial tissue, whereas permeability of urine to the mesenchymal layer will result in greater proliferation of that tissue. This could be supported by the fact that urine contains large amounts of EGF-related mitogens (Lakshmanan, et al. 1990) that could potentially stimulate proliferation in either the epithelial layer or the mesenchymal layer depending on the depth of urine penetrance. EGFR signaling mediates urothelial regeneration (Daher, et al. 2003), making it a likely candidate to explain overproliferation following urine exposure.

The exocyst may traffic EGFR to the surface of urothelial cells (Fogelgren, et al. 2014). Since UPK KO models do not affect exocyst function, EGFR signaling will be intact and it is possible that this causes the overproliferation of urothelium. But since exocyst function in Sec10 CKOs is lost only in the urothelium, this could result in no urothelial response but intact EGFR signaling and subsequent overproliferation of the underlying mesenchyme.

Claudin Knockout Mouse Model

Claudin4 (Cldn4) knockout mice experience urothelial hyperplasia with hydronephrosis development usually around 12 months (Fujita, et al. 2012). Even though Cldn4 is found in tight junctions (TJs), other claudins were found to compensate to maintain normal numbers and localization of TJs. Expression of claudins is unaffected; change in localization mediates the compensatory response.

Perhaps these compensatory claudins are less effective at maintaining barrier function. Uroplakins are unaffected, indicating UPKs do not compensate for this potential loss of barrier integrity. A possible explanation is that claudin compensation causes minimal damage to barrier function, resulting in a similar response as UPK KO models, but with a slower development due to the fact that UPK KO ureter urothelium has greater barrier impermeability to urine to initiate EGFR mediated proliferation.

Δ Np63 Knockout Mouse Model

P63 is essential for proliferation of progenitor cells in stratified epithelia. Knockout of p63 during development results in loss of stratified epithelium (Senoo, et al. 2007). Δ Np63, an isoform of the transcription factor p63, is detected during normal urothelial differentiation, predominantly in the basal and intermediate layers of ureter urothelium.

When Δ Np63 is knocked out of the developing ureter urothelium, the urothelium fails to stratify, but is still able to express terminal differentiation markers (Weiss, et al. 2013). P63 knockout ureter urothelium still is able to differentiate. These mice do not develop ureter obstructions or hydronephrosis, consistent with our findings that impaired urothelial differentiation can lead to obstruction formation. The major effect of p63 KO is likely a loss of regenerative capability.

Sec10-CKO ureters start to lose p63 positive urothelial cells at E17.5. Given the phenotype of Δ Np63 KO ureter urothelium, it is clear that the development of the UPJ obstruction is not due to loss of p63 cell so much as loss of terminally differentiated urothelial cells.

PPAR γ Knockout Mouse Model

PPAR γ is the upstream regulator of UPK expression. When PPAR γ is knocked out of the development of UB-derived structures, ureters have abnormal infoldings of the basal urothelial layer, and occasionally develop hydroureter (Weiss, et al. 2013). Molecular analyses seem to suggest that the apical cells of these knockout ureters behave like basal cells, with increased Shh expression and decreased UPK expression.

Because PPAR γ can only function as a transcription factor when there is accompanying retinoic acid (RA) signaling, it is interesting to also consider the RA signaling knock-down mouse model. RA knock-down results in impaired differentiation of I and S cells during development; B cell development is RA-independent (Gandhi, et al. 2013). This may explain why apical cells in PPAR γ knockout urothelial cells are more basal-like; PPAR γ /RA signaling can override the basal cell differentiation program in favor of superficial cell differentiation. This would suggest another differentiation signal for urothelial differentiation that is modified by PPAR γ selectively in the apical cells.

Therefore, it is likely that the apical cells of PPAR γ KO urothelium will allow some permeability, and yet there was no mesenchymal overgrowth (like Sec10-CKOs), nor epithelial overgrowth (like Cldn4 and UPK knockout models).

It would make sense that PPAR γ KO urothelium will have at least as much permeability to urine as UPK KO models, or more permeability considering PPAR γ also increases expression of TJ proteins (Varley and Southgate 2008). This raises the question: why do PPAR γ KO ureters have no overgrowth of either cell type? It is known that urothelial differentiation requires both PPAR γ activation and inhibition of the EGFR pathway (Varley and Southgate 2008). The permeation of EGF-related mitogens from urine might further impair urothelial differentiation. PPAR γ is also a known suppressor of urothelial proliferation (Kawakami, et al. 2002). But if UPK KO models have normal PPAR γ expression, why do they have overproliferation of urothelium? And why do PPAR γ KOs have no overproliferation? A possible explanation is that PPAR γ KO apical cells are more basal-like in molecular make-up that may (a) provide enough of a barrier to prevent urine to permeate into the mesenchymal layer, and (b) not express EGFR. In the

future, I would like to stain for EGFR to determine if this explanation is possible. I tried various protocols but was unsuccessful in staining ureter sections for EGFR to determine if it is only expressed in certain cell types normally, and if EGFR expression and/or localization is defective in Sec10-CKOs.

Brg1 Knockout Mouse Model

Mice with a conditional knocked out of Brg1 only in UB derived structures will develop hydronephrosis by 3 weeks of age (Weiss, et al. 2013). Interestingly, these mice experience several similarities in gene expression as our Sec10-CKOs: decreased PPAR γ and UPKs. This means that terminal urothelial differentiation is impaired, and likely the functional barrier will have increased permeability. These ureters do not have mesenchymal nor epithelial overgrowth. Instead, these mice developed hydronephrosis due to a decreased smooth muscle layer, from decreased Shh expression. For the most part, Brg1 KO ureters are very similar to PPAR γ KOs, with the difference that 100% of Brg1 KOs develop hydronephrosis compared to only about 7.7% in PPAR γ KOs.

Brg1 regulates not only PPAR γ expression for terminal proliferation, but also p63 expression for basal cell self renewal. Brg1 KO ureters will differ from PPAR γ KO ureters in that there will be almost no p63-positive cells. This could explain why at birth, Brg1 KO urothelium will remain a monolayer while PPAR γ KO ureters are stratified, albeit with impaired differentiation.

Hydronephrosis for both Brg1 and PPAR γ KOs is secondary to impaired SMC differentiation, resulting from decreased Shh signaling from the urothelium. It has been proposed that p63 can induce Shh expression (Caserta, et al. 2006). Therefore, the difference in penetrance of the hydronephrosis phenotype can be explained by the amount of Shh expression: Brg1 KO mice have a decrease in Shh mediated not only by the loss of PPAR γ but also by p63. Note that Weiss et al. report no change in Shh expression in p63 KO ureters, however this conclusion does not appear to be supported; in my opinion, p63 KO ureter sections appear to have less Shh staining, and Shh expression quantification and statistical significance was not reported. Therefore, I believe Shh alone is a strong potential candidate to explain the difference between Brg1 KO and PPAR γ KO hydronephrosis development.

In this case, hydroureter is due to a “functional” obstruction caused by underdevelopment or dysfunction of the smooth muscle layer. Smooth muscle impairment can cause urine to build up in the renal pelvis, not due to a physical obstruction, but due to the lack of peristalsis and the propulsion of urine from the kidney to the bladder. There are several other mouse models that have been shown to cause functional obstructions. To focus on the development of the Sec10-CKO obstruction, I will only discuss one of these genetic mouse models.

Tbx18 Knockout Mouse Model

T-box transcription factor Tbx18 is expressed in the undifferentiated mesenchyme around the ureter. A global Tbx18 KO mouse shows various anomalies across different organ systems; analysis of the urinary tract reveals hydronephrosis at birth with UPJ functional obstruction (Airik, et al. 2006). As expected, loss of Tbx18 results in reduced proliferation and differentiation of smooth muscle, and in hydronephrosis. However, the reason I believe this model may be of importance is because there is also an effect on the urothelium: uroplakin expression was very weak and there was decreased urothelial proliferation. Because Tbx18 expression has only been reported in the mesenchymal fate to form peristaltic machinery, this implicates Tbx18 as part of a signaling pathway from the underlying mesenchyme that influences urothelial development. If this is true, then this opens the door to a new, unexplored signaling pathway influencing urothelial development. A portion of this pathway, perhaps a surface receptor, may be trafficked by the exocyst.

If Tbx18 regulates urothelial proliferation through a signaling pathway involving exocyst function, this could explain why there is a disappearance of urothelial cells in Sec10-CKO ureters following urine exposure when UPK KO mice experience urothelial over-proliferation. Loss of this mesenchymal-urothelial communication would impair the regenerative capabilities of the urothelium.

Follow-up experiments show that urothelial signals are required to maintain Tbx18 expression in the ureter and to suppress renal stromal fate of Tbx18-positive cells (Bohnenpoll, et al. 2013). These experiments, conducted around E11.5-E12.5, showed that ureter urothelium was

required for Tbx18-positive cells to acquire ureteric fate; without ureter urothelium present, these cells migrate to the kidney. If this urothelium-mesenchyme signaling is mediated by the exocyst, it could lead to an increase in fibroblast-like cells derived from the Tbx18+ cells.

Significance and Clinical Relevance

Our findings suggest Sec10-CKO urothelia fails to differentiate, leading to functional barrier impairment; then, a fibrotic wound healing response initiates shortly after the start of urine production. It is prudent to determine if any of these same findings have been found in human UPJ obstructions.

The hypothesis that urothelial damage causes UPJ obstructions was first proposed in 1995, in a study that analyzed on the UPJ pyeloplasty samples from infants (Bartoli, et al. 1996). They found that UPJ obstruction sections showed regions of the luminal surface of the ureter lacked epithelial cells, and predicted these epithelial breaks allowed for urine damage. Their publication not only supports our findings, but predicts some of them, like impaired urothelial barrier as a cause for structural changes leading to fibrotic stenosis.

We found increased expression of fibrotic wound healing markers, including TGF β 1, Collagen IV, SMA, Periostin and S100A4. Human analyses have also detected increases in TGF β (Yang, et al. 2006), collagen (Decramer, et al. 2006), and SMA (Murer, et al. 2006). We found decrease expression of several proteins important for urothelial differentiation, including uroplakins and PPAR γ . I was unable to find any published proteomic analysis for these proteins in human samples.

These data support Sec10 as a good model for human UPJ obstruction development; however, future protein analyses on human tissue will be necessary to determine if the fibrotic wound healing response is secondary to immature urothelia lacking a strong functional urothelial barrier, or some other cause.

Conclusion

In conclusion, our hypothesis that Sec10-CKOs have disrupted urothelial barrier formation that leads to fibrotic response that obstructs the UPJ was supported.

Urothelium of the UPJ differentiates later than the urothelia in other organs. If urothelial differentiation is impaired or delayed by Sec10 loss when urine production starts, around E16.5, urine will permeate and damage the more vulnerable UPJ region more often than other portions of the ureter. Toxic factors provide another means in which urine can injure urothelia and increase permeability at the functional barrier. Therefore, by better understanding the development of UPJ obstruction in Sec10-CKO, we may be able to better understand the genetic and/or environmental factors that increase risk for UPJ obstruction formation.

Our study shows the key fibrotic mediator, TGF β 1, is greatly upregulated, fibroblasts are activated, and there is evidence of stromal remodeling. These are hallmarks of granulation tissue and provide strong support that Sec10-CKO mice undergo a fibrotic wound healing response following the onset of urine production. It is yet to be determined how much canonical TGF β pathways and non-canonical pathways contribute to the development of UPJ obstructions in Sec10-CKOs.

Studies of other genetic mouse models provide insight as to possible mechanisms driving UPJ obstructions in our Sec10-CKO mouse. We know other mice with an impaired functional barrier (ie. uroplakin, claudin, and PPAR γ knockout mice) do not yield as severe of a phenotype. I propose that permeability of urine will allow cells to be exposed to the EGF-related mitogens in urine and that models with more permeability will have deeper tissues to over-proliferate and contribute to the formation of the obstruction. It has been suggested that the exocyst is important for EGFR signaling. I predict that loss of the exocyst (and EGFR signaling) in urothelial cells results in the absence of over-proliferation of these cells when exposed to urine, but other cell types, like mesenchymal cells, still over-proliferate in response to exposure to the EGF-related mitogens in urine.

Genetic mouse models of Tbx18 propose a second potential mode of operation for the Sec10-CKO phenotype. Tbx18 is expressed in the developing ureter mesenchyme and affects not only

the development of the smooth muscle layer but also affects urothelial differentiation. There must be some signaling event between these two cell types that is in some part regulated by Tbx18. This signaling even is another potential candidate for exocyst function.

Current human studies of UPJ obstructions appear to show similar fibrotic signaling events as our Sec10-CKO mouse. Next, we would like to study human UPJ obstruction sites to see if they also appear to have markers indicative of poor differentiation. These results would lend further support that our mouse model is highly relevant and a strong tool to study human UPJ obstruction development.

This mouse model will have a profound impact on how we study the development of prenatal UPJ obstructions. These results give exciting new insight in the development of this condition that give hope to find ways to prevent and/or treat this condition.

References

- Airik, R., et al. 2006. "Tbx18 Regulates the Development of the Ureteral Mesenchyme." *J Clin Invest* 116, no. 3 (Mar): 663-74. <http://dx.doi.org/10.1172/jci26027>.
- Andersen, N. J., and C. Yeaman. 2010. "Sec3-Containing Exocyst Complex Is Required for Desmosome Assembly in Mammalian Epithelial Cells." *Mol Biol Cell* 21, no. 1 (Jan 1): 152-64. <http://dx.doi.org/10.1091/mbc.E09-06-0459>.
- Bartoli, F. A., et al. 1996. "Urothelium Damage as the Primary Cause of Ureteropelvic Junction Obstruction: A New Hypothesis." *Urol Res* 24, no. 1: 9-13.
- Baum, J., and H. S. Duffy. 2011. "Fibroblasts and Myofibroblasts: What Are We Talking About?" *J Cardiovasc Pharmacol* 57, no. 4 (Apr): 376-9. <http://dx.doi.org/10.1097/FJC.0b013e3182116e39>.
- Benfield, M. R., et al. 2003. "Changing Trends in Pediatric Transplantation: 2001 Annual Report of the North American Pediatric Renal Transplant Cooperative Study." *Pediatr Transplant* 7, no. 4 (Aug): 321-35.
- Bock, M., et al. 2014. "Identification of Elf3 as an Early Transcriptional Regulator of Human Urothelium." *Dev Biol* 386, no. 2 (Feb 15): 321-30. <http://dx.doi.org/10.1016/j.ydbio.2013.12.028>.
- Bohnenpoll, T., et al. 2013. "Tbx18 Expression Demarcates Multipotent Precursor Populations in the Developing Urogenital System but Is Exclusively Required within the Ureteric Mesenchymal Lineage to Suppress a Renal Stromal Fate." *Dev Biol* 380, no. 1 (Aug 1): 25-36. <http://dx.doi.org/10.1016/j.ydbio.2013.04.036>.
- Bohnenpoll, T., and A. Kispert. 2014. "Ureter Growth and Differentiation." *Semin Cell Dev Biol* 36 (Dec): 21-30. <http://dx.doi.org/10.1016/j.semcdb.2014.07.014>.
- Bondi, C. D., et al. 2010. "Nad(P)H Oxidase Mediates Tgf-Beta1-Induced Activation of Kidney Myofibroblasts." *J Am Soc Nephrol* 21, no. 1 (Jan): 93-102. <http://dx.doi.org/10.1681/asn.2009020146>.
- Brenner-Anantharam, A., et al. 2007. "Tailbud-Derived Mesenchyme Promotes Urinary Tract Segmentation Via Bmp4 Signaling." *Development* 134, no. 10 (May): 1967-75. <http://dx.doi.org/10.1242/dev.004234>.
- Bryant, D. M., et al. 2010. "A Molecular Network for De Novo Generation of the Apical Surface and Lumen." *Nat Cell Biol* 12, no. 11 (Nov): 1035-45. <http://dx.doi.org/10.1038/ncb2106>.
- Bultman, S., et al. 2000. "A Brg1 Null Mutation in the Mouse Reveals Functional Differences among Mammalian Swi/Snf Complexes." *Mol Cell* 6, no. 6 (Dec): 1287-95.
- Carlson, M., and B. C. Laurent. 1994. "The Snf/Swi Family of Global Transcriptional Activators." *Curr Opin Cell Biol* 6, no. 3 (Jun): 396-402.
- Caserta, T. M., et al. 2006. "P63 Overexpression Induces the Expression of Sonic Hedgehog." *Mol Cancer Res* 4, no. 10 (Oct): 759-68. <http://dx.doi.org/10.1158/1541-7786.mcr-05-0149>.
- Caubit, X., et al. 2008. "Teashirt 3 Is Necessary for Ureteral Smooth Muscle Differentiation Downstream of Shh and Bmp4." *Development* 135, no. 19 (Oct): 3301-10. <http://dx.doi.org/10.1242/dev.022442>.
- Chen, Y., et al. 2003. "Rab27b Is Associated with Fusiform Vesicles and May Be Involved in Targeting Uroplakins to Urothelial Apical Membranes." *Proc Natl Acad Sci U S A* 100, no. 24 (Nov): 14012-7. <http://dx.doi.org/10.1073/pnas.2436350100>.

- Crawford, J., et al. 2015. "Periostin Induces Fibroblast Proliferation and Myofibroblast Persistence in Hypertrophic Scarring." *Exp Dermatol* 24, no. 2 (Feb): 120-6. <http://dx.doi.org/10.1111/exd.12601>.
- Daher, A., et al. 2003. "Epidermal Growth Factor Receptor Regulates Normal Urothelial Regeneration." *Lab Invest* 83, no. 9 (Sep): 1333-41.
- Davidson, A. J. 2008. "Mouse Kidney Development." In *Stembook*. Cambridge (MA): Harvard Stem Cell Institute Copyright: (c) 2008 Alan J. Davidson.
- Decramer, S., et al. 2006. "Predicting the Clinical Outcome of Congenital Unilateral Ureteropelvic Junction Obstruction in Newborn by Urinary Proteome Analysis." *Nat Med* 12, no. 4 (Apr): 398-400. <http://dx.doi.org/10.1038/nm1384>.
- Derynck, R., and Y. E. Zhang. 2003. "Smad-Dependent and Smad-Independent Pathways in Tgf-Beta Family Signalling." *Nature* 425, no. 6958 (Oct 9): 577-84. <http://dx.doi.org/10.1038/nature02006>.
- Diep, C. Q., et al. 2015. "Development of the Zebrafish Mesonephros." *Genesis* 53, no. 3-4 (Mar-Apr): 257-69. <http://dx.doi.org/10.1002/dvg.22846>.
- Diez-Marques, L., et al. 2002. "Expression of Endoglin in Human Mesangial Cells: Modulation of Extracellular Matrix Synthesis." *Biochim Biophys Acta* 1587, no. 1 (May 21): 36-44.
- Dressler, G. R. 2009. "Advances in Early Kidney Specification, Development and Patterning." *Development* 136, no. 23 (Dec): 3863-74. <http://dx.doi.org/10.1242/dev.034876>.
- Duan, W. J., et al. 2014. "Opposing Roles for Smad2 and Smad3 in Peritoneal Fibrosis in Vivo and in Vitro." *Am J Pathol* 184, no. 8 (Aug): 2275-84. <http://dx.doi.org/10.1016/j.ajpath.2014.04.014>.
- Elliott, C. G., et al. 2012. "Periostin Modulates Myofibroblast Differentiation During Full-Thickness Cutaneous Wound Repair." *J Cell Sci* 125, no. Pt 1 (Jan 1): 121-32. <http://dx.doi.org/10.1242/jcs.087841>.
- Eyden, B. 2008. "The Myofibroblast: Phenotypic Characterization as a Prerequisite to Understanding Its Functions in Translational Medicine." *J Cell Mol Med* 12, no. 1 (Jan-Feb): 22-37. <http://dx.doi.org/10.1111/j.1582-4934.2007.00213.x>.
- Fischer, A. H., et al. 2008. "Hematoxylin and Eosin Staining of Tissue and Cell Sections." *CSH Protoc* 2008: pdb.prot4986. <http://dx.doi.org/10.1101/pdb.prot4986>.
- Fogelgren, B., et al. 2015. "Urothelial Defects from Targeted Inactivation of Exocyst Sec10 in Mice Cause Ureteropelvic Junction Obstructions." *PLoS One* 10, no. 6: e0129346. <http://dx.doi.org/10.1371/journal.pone.0129346>.
- . 2009. "Deficiency in Six2 During Prenatal Development Is Associated with Reduced Nephron Number, Chronic Renal Failure, and Hypertension in Br/+ Adult Mice." *Am J Physiol Renal Physiol* 296, no. 5 (May): F1166-78. <http://dx.doi.org/10.1152/ajprenal.90550.2008>.
- . 2014. "Exocyst Sec10 Protects Renal Tubule Cells from Injury by Egfr/Mapk Activation and Effects on Endocytosis." *Am J Physiol Renal Physiol* 307, no. 12 (Dec 15): F1334-41. <http://dx.doi.org/10.1152/ajprenal.00032.2014>.

- Friedrich, G. A., J. D. Hildebrand, and P. Soriano. 1997. "The Secretory Protein Sec8 Is Required for Paraxial Mesoderm Formation in the Mouse." *Dev Biol* 192, no. 2 (Dec 15): 364-74. <http://dx.doi.org/10.1006/dbio.1997.8727>.
- Fujita, H., et al. 2012. "Claudin-4 Deficiency Results in Urothelial Hyperplasia and Lethal Hydronephrosis." *PLoS One* 7, no. 12: e52272. <http://dx.doi.org/10.1371/journal.pone.0052272>.
- Gandhi, D., et al. 2013. "Retinoid Signaling in Progenitors Controls Specification and Regeneration of the Urothelium." *Dev Cell* 26, no. 5 (Sep 16): 469-82. <http://dx.doi.org/10.1016/j.devcel.2013.07.017>.
- Gunn, T. R., J. D. Mora, and P. Pease. 1995. "Antenatal Diagnosis of Urinary Tract Abnormalities by Ultrasonography after 28 Weeks' Gestation: Incidence and Outcome." *Am J Obstet Gynecol* 172, no. 2 Pt 1 (Feb): 479-86.
- Guo, W., et al. 1999. "The Exocyst Is an Effector for Sec4p, Targeting Secretory Vesicles to Sites of Exocytosis." *Embo j* 18, no. 4 (Feb 15): 1071-80. <http://dx.doi.org/10.1093/emboj/18.4.1071>.
- Hazelett, C. C., D. Sheff, and C. Yeaman. 2011. "Rala and Ralb Differentially Regulate Development of Epithelial Tight Junctions." *Mol Biol Cell* 22, no. 24 (Dec): 4787-800. <http://dx.doi.org/10.1091/mbc.E11-07-0657>.
- Hu, P., et al. 2000. "Ablation of Uroplakin Iii Gene Results in Small Urothelial Plaques, Urothelial Leakage, and Vesicoureteral Reflux." *J Cell Biol* 151, no. 5 (Nov 27): 961-72.
- . 2002. "Role of Membrane Proteins in Permeability Barrier Function: Uroplakin Ablation Elevates Urothelial Permeability." *Am J Physiol Renal Physiol* 283, no. 6 (Dec): F1200-7. <http://dx.doi.org/10.1152/ajprenal.00043.2002>.
- Inoue, T., et al. 2001. "Regulation of Fibronectin Expression and Splicing in Migrating Epithelial Cells: Migrating Mdkc Cells Produce a Lesser Amount of, but More Active, Fibronectin." *Biochem Biophys Res Commun* 280, no. 5 (Feb 9): 1262-8. <http://dx.doi.org/10.1006/bbrc.2001.4264>.
- Jain, M., et al. 2013. "Mitochondrial Reactive Oxygen Species Regulate Transforming Growth Factor-Beta Signaling." *J Biol Chem* 288, no. 2 (Jan 11): 770-7. <http://dx.doi.org/10.1074/jbc.M112.431973>.
- Jost, S. P. 1986. "Renewal of Normal Urothelium in Adult Mice." *Virchows Arch B Cell Pathol Incl Mol Pathol* 51, no. 1: 65-70.
- Kawai, T., et al. 2009. "Ppar-Gamma Agonist Attenuates Renal Interstitial Fibrosis and Inflammation through Reduction of Tgf-Beta." *Lab Invest* 89, no. 1 (Jan): 47-58. <http://dx.doi.org/10.1038/labinvest.2008.104>.
- Kawakami, S., et al. 2002. "Ppargamma Ligands Suppress Proliferation of Human Urothelial Basal Cells in Vitro." *J Cell Physiol* 191, no. 3 (Jun): 310-9. <http://dx.doi.org/10.1002/jcp.10099>.
- Keller, H., et al. 1993. "Fatty Acids and Retinoids Control Lipid Metabolism through Activation of Peroxisome Proliferator-Activated Receptor-Retinoid X Receptor Heterodimers." *Proc Natl Acad Sci U S A* 90, no. 6 (Mar 15): 2160-4.
- Khandelwal, P., et al. 2008. "Rab11a-Dependent Exocytosis of Discoidal/Fusiform Vesicles in Bladder Umbrella Cells." *Proc Natl Acad Sci U S A* 105, no. 41 (Oct 14): 15773-8. <http://dx.doi.org/10.1073/pnas.0805636105>.
- Klein, J., et al. 2011. "Congenital Ureteropelvic Junction Obstruction: Human Disease and Animal Models." *Int J Exp Pathol* 92, no. 3 (Jun): 168-92. <http://dx.doi.org/10.1111/j.1365-2613.2010.00727.x>.

- Kliwer, S. A., et al. 1992. "Convergence of 9-Cis Retinoic Acid and Peroxisome Proliferator Signalling Pathways through Heterodimer Formation of Their Receptors." *Nature* 358, no. 6389 (Aug 27): 771-4. <http://dx.doi.org/10.1038/358771a0>.
- Kong, X. T., et al. 2004. "Roles of Uroplakins in Plaque Formation, Umbrella Cell Enlargement, and Urinary Tract Diseases." *J Cell Biol* 167, no. 6 (Dec): 1195-204. <http://dx.doi.org/10.1083/jcb.200406025>.
- Kuure, S., R. Vuolteenaho, and S. Vainio. 2000. "Kidney Morphogenesis: Cellular and Molecular Regulation." *Mech Dev* 92, no. 1 (Mar 15): 31-45.
- Lakshmanan, J., et al. 1990. "Identification of Pro-Epidermal Growth Factor and High Molecular Weight Epidermal Growth Factors in Adult Mouse Urine." *Biochem Biophys Res Commun* 173, no. 3 (Dec 31): 902-11.
- Langevin, J., et al. 2005. "Drosophila Exocyst Components Sec5, Sec6, and Sec15 Regulate De-Cadherin Trafficking from Recycling Endosomes to the Plasma Membrane." *Dev Cell* 9, no. 3 (Sep): 365-76.
- Leask, A., and D. J. Abraham. 2004. "Tgf-Beta Signaling and the Fibrotic Response." *Faseb j* 18, no. 7 (May): 816-27. <http://dx.doi.org/10.1096/fj.03-1273rev>.
- Liang, F. X., et al. 2005. "Cellular Basis of Urothelial Squamous Metaplasia: Roles of Lineage Heterogeneity and Cell Replacement." *J Cell Biol* 171, no. 5 (Dec 5): 835-44. <http://dx.doi.org/10.1083/jcb.200505035>.
- Liu, R. M., and L. P. Desai. 2015. "Reciprocal Regulation of Tgf-Beta and Reactive Oxygen Species: A Perverse Cycle for Fibrosis." *Redox Biol* 6 (Dec): 565-77. <http://dx.doi.org/10.1016/j.redox.2015.09.009>.
- Livera, L. N., et al. 1989. "Antenatal Ultrasonography to Detect Fetal Renal Abnormalities: A Prospective Screening Programme." *Bmj* 298, no. 6685 (May 27): 1421-3.
- Madisen, L., et al. 2010. "A Robust and High-Throughput Cre Reporting and Characterization System for the Whole Mouse Brain." *Nat Neurosci* 13, no. 1 (Jan): 133-40. <http://dx.doi.org/10.1038/nn.2467>.
- Massague, J., and D. Wotton. 2000. "Transcriptional Control by the Tgf-Beta/Smad Signaling System." *Embo j* 19, no. 8 (Apr 17): 1745-54. <http://dx.doi.org/10.1093/emboj/19.8.1745>.
- Mathews, G. A., and C. Ffrench-Constant. 1995. "Embryonic Fibronectins Are up-Regulated Following Peripheral Nerve Injury in Rats." *J Neurobiol* 26, no. 2 (Feb): 171-88. <http://dx.doi.org/10.1002/neu.480260203>.
- Meng, X. M., et al. 2010. "Smad2 Protects against Tgf-Beta/Smad3-Mediated Renal Fibrosis." *J Am Soc Nephrol* 21, no. 9 (Sep): 1477-87. <http://dx.doi.org/10.1681/asn.2009121244>.
- Munoz-Felix, J. M., et al. 2015. "Tgf-Beta/Bmp Proteins as Therapeutic Targets in Renal Fibrosis. Where Have We Arrived after 25 Years of Trials and Tribulations?" *Pharmacol Ther* 156 (Dec): 44-58. <http://dx.doi.org/10.1016/j.pharmthera.2015.10.003>.
- Murer, L., et al. 2006. "Clinical and Molecular Markers of Chronic Interstitial Nephropathy in Congenital Unilateral Ureteropelvic Junction Obstruction." *J Urol* 176, no. 6 Pt 1 (Dec): 2668-73; discussion 2673. <http://dx.doi.org/10.1016/j.juro.2006.08.055>.
- Muro, A. F., et al. 2003. "Regulated Splicing of the Fibronectin Eda Exon Is Essential for Proper Skin Wound Healing and Normal Lifespan." *J Cell Biol* 162, no. 1 (Jul 7): 149-60. <http://dx.doi.org/10.1083/jcb.200212079>.

- . 2008. "An Essential Role for Fibronectin Extra Type Iii Domain a in Pulmonary Fibrosis." *Am J Respir Crit Care Med* 177, no. 6 (Mar 15): 638-45. <http://dx.doi.org/10.1164/rccm.200708-1291OC>.
- Murthy, M., et al. 2003. "Mutations in the Exocyst Component Sec5 Disrupt Neuronal Membrane Traffic, but Neurotransmitter Release Persists." *Neuron* 37, no. 3 (Feb 6): 433-47.
- . 2005. "Sec6 Mutations and the Drosophila Exocyst Complex." *J Cell Sci* 118, no. Pt 6 (Mar 15): 1139-50. <http://dx.doi.org/10.1242/jcs.01644>.
- Mysorekar, I. U., et al. 2002. "Molecular Regulation of Urothelial Renewal and Host Defenses During Infection with Uropathogenic Escherichia Coli." *J Biol Chem* 277, no. 9 (Mar 1): 7412-9. <http://dx.doi.org/10.1074/jbc.M110560200>.
- Nguyen, H. T., et al. 2010. "The Society for Fetal Urology Consensus Statement on the Evaluation and Management of Antenatal Hydronephrosis." *J Pediatr Urol* 6, no. 3 (Jun): 212-31. <http://dx.doi.org/10.1016/j.jpuro.2010.02.205>.
- Parsons, C. L., et al. 2000. "Cyto-Injury Factors in Urine: A Possible Mechanism for the Development of Interstitial Cystitis." *J Urol* 164, no. 4 (Oct): 1381-4.
- . 2007. "Defective Tamm-Horsfall Protein in Patients with Interstitial Cystitis." *J Urol* 178, no. 6 (Dec): 2665-70. <http://dx.doi.org/10.1016/j.juro.2007.07.125>.
- Paulsson, M. 1992. "Basement Membrane Proteins: Structure, Assembly, and Cellular Interactions." *Crit Rev Biochem Mol Biol* 27, no. 1-2: 93-127. <http://dx.doi.org/10.3109/10409239209082560>.
- Qi, C., Y. Zhu, and J. K. Reddy. 2000. "Peroxisome Proliferator-Activated Receptors, Coactivators, and Downstream Targets." *Cell Biochem Biophys* 32 Spring: 187-204.
- Rajasekaran, M., P. Stein, and C. L. Parsons. 2006. "Toxic Factors in Human Urine That Injure Urothelium." *Int J Urol* 13, no. 4 (Apr): 409-14. <http://dx.doi.org/10.1111/j.1442-2042.2006.01301.x>.
- Rasouly, H. M., and W. Lu. 2013. "Lower Urinary Tract Development and Disease." *Wiley Interdiscip Rev Syst Biol Med* 5, no. 3 (May-Jun): 307-42. <http://dx.doi.org/10.1002/wsbm.1212>.
- Rogers, K. K., et al. 2004. "The Exocyst Localizes to the Primary Cilium in Mdkc Cells." *Biochem Biophys Res Commun* 319, no. 1 (Jun 18): 138-43. <http://dx.doi.org/10.1016/j.bbrc.2004.04.165>.
- Sairam, S., et al. 2001. "Natural History of Fetal Hydronephrosis Diagnosed on Mid-Trimester Ultrasound." *Ultrasound Obstet Gynecol* 17, no. 3 (Mar): 191-6. <http://dx.doi.org/10.1046/j.1469-0705.2001.00333.x>.
- Sato, M., et al. 2003. "Targeted Disruption of Tgf-Beta1/Smad3 Signaling Protects against Renal Tubulointerstitial Fibrosis Induced by Unilateral Ureteral Obstruction." *J Clin Invest* 112, no. 10 (Nov): 1486-94. <http://dx.doi.org/10.1172/jci19270>.
- Schneeberger, E. E., and R. D. Lynch. 2004. "The Tight Junction: A Multifunctional Complex." *Am J Physiol Cell Physiol* 286, no. 6 (Jun): C1213-28. <http://dx.doi.org/10.1152/ajpcell.00558.2003>.
- Senoo, M., et al. 2007. "P63 Is Essential for the Proliferative Potential of Stem Cells in Stratified Epithelia." *Cell* 129, no. 3 (May 4): 523-36. <http://dx.doi.org/10.1016/j.cell.2007.02.045>.
- Serini, G., et al. 1998. "The Fibronectin Domain Ed-a Is Crucial for Myofibroblastic Phenotype Induction by Transforming Growth Factor-Beta1." *J Cell Biol* 142, no. 3 (Aug 10): 873-81.

- Seufert, D. W., et al. 1999. "Developmental Basis of Pronephric Defects in Xenopus Body Plan Phenotypes." *Dev Biol* 215, no. 2 (Nov 15): 233-42. <http://dx.doi.org/10.1006/dbio.1999.9476>.
- Shao, X., et al. 2002. "A Minimal Ksp-Cadherin Promoter Linked to a Green Fluorescent Protein Reporter Gene Exhibits Tissue-Specific Expression in the Developing Kidney and Genitourinary Tract." *J Am Soc Nephrol* 13, no. 7 (Jul): 1824-36.
- Shao, X., S. Somlo, and P. Igarashi. 2002. "Epithelial-Specific Cre/Lox Recombination in the Developing Kidney and Genitourinary Tract." *J Am Soc Nephrol* 13, no. 7 (Jul): 1837-46.
- Skalli, O., et al. 1989. "Myofibroblasts from Diverse Pathologic Settings Are Heterogeneous in Their Content of Actin Isoforms and Intermediate Filament Proteins." *Lab Invest* 60, no. 2 (Feb): 275-85.
- Smith, Homer William. 1959. *From Fish to Philosopher: The Story of Our Internal Environment*: CIBA Pharmaceutical Products Inc.
- Smith, N. J., et al. 2015. "The Human Urothelial Tight Junction: Claudin 3 and the Zo-1alpha Switch." *Bladder (San Franc)* 2, no. 1: e9. <http://dx.doi.org/10.14440/bladder.2015.33>.
- Theiler, Karl. 2013. *The House Mouse: Atlas of Embryonic Development*: Springer Science & Business Media.
- Trowe, M. O., et al. 2012. "Canonical Wnt Signaling Regulates Smooth Muscle Precursor Development in the Mouse Ureter." *Development* 139, no. 17 (Sep): 3099-108. <http://dx.doi.org/10.1242/dev.077388>.
- Truschel, S. T., et al. 2002. "Stretch-Regulated Exocytosis/Endocytosis in Bladder Umbrella Cells." *Mol Biol Cell* 13, no. 3 (Mar): 830-46. <http://dx.doi.org/10.1091/mbc.01-09-0435>.
- Tu, L., T. T. Sun, and G. Kreibich. 2002. "Specific Heterodimer Formation Is a Prerequisite for Uroplakins to Exit from the Endoplasmic Reticulum." *Mol Biol Cell* 13, no. 12 (Dec): 4221-30. <http://dx.doi.org/10.1091/mbc.E02-04-0211>.
- Urine Blockage in Newborns*. 2006. NIH: Clearinghouse NIOKaUDI.
- Valles, P. G., et al. 2003. "Role of Endogenous Nitric Oxide in Unilateral Ureteropelvic Junction Obstruction in Children." *Kidney Int* 63, no. 3 (Mar): 1104-15. <http://dx.doi.org/10.1046/j.1523-1755.2003.00833.x>.
- Varley, C., et al. 2005. "Autocrine Regulation of Human Urothelial Cell Proliferation and Migration During Regenerative Responses in Vitro." *Exp Cell Res* 306, no. 1 (May 15): 216-29. <http://dx.doi.org/10.1016/j.yexcr.2005.02.004>.
- Varley, C. L., et al. 2009. "Foxa1 and Irf-1 Intermediary Transcriptional Regulators of Ppargamma-Induced Urothelial Cytodifferentiation." *Cell Death Differ* 16, no. 1 (Jan): 103-14. <http://dx.doi.org/10.1038/cdd.2008.116>.
- Varley, C. L., and J. Southgate. 2008. "Effects of Ppar Agonists on Proliferation and Differentiation in Human Urothelium." *Exp Toxicol Pathol* 60, no. 6 (Sep): 435-41. <http://dx.doi.org/10.1016/j.etp.2008.04.009>.
- Varley, C. L., et al. 2004. "Role of Ppargamma and Egfr Signalling in the Urothelial Terminal Differentiation Programme." *J Cell Sci* 117, no. Pt 10 (Apr): 2029-36. <http://dx.doi.org/10.1242/jcs.01042>.

- Wankel, B., et al. 2016. "Sequential and Compartmentalized Action of Rab5, Snare and Mal in the Apical Delivery of Fusiform Vesicles in Urothelial Umbrella Cells." *Mol Biol Cell* (Mar 23). <http://dx.doi.org/10.1091/mbc.E15-04-0230>.
- Wei, J., et al. 2012. "Regulation of Matrix Remodeling by Peroxisome Proliferator-Activated Receptor-Gamma: A Novel Link between Metabolism and Fibrogenesis." *Open Rheumatol J* 6: 103-15. <http://dx.doi.org/10.2174/1874312901206010103>.
- Weiss, R. M., et al. 2013. "Brg1 Determines Urothelial Cell Fate During Ureter Development." *J Am Soc Nephrol* 24, no. 4 (Mar): 618-26. <http://dx.doi.org/10.1681/ASN.2012090902>.
- Wu, B., and W. Guo. 2015. "The Exocyst at a Glance." *J Cell Sci* 128, no. 16 (Aug 15): 2957-64. <http://dx.doi.org/10.1242/jcs.156398>.
- Wu, X. R., et al. 2009. "Uroplakins in Urothelial Biology, Function, and Disease." *Kidney Int* 75, no. 11 (Jun): 1153-65. <http://dx.doi.org/10.1038/ki.2009.73>.
- . 1994. "Mammalian Uroplakins. A Group of Highly Conserved Urothelial Differentiation-Related Membrane Proteins." *J Biol Chem* 269, no. 18 (May 6): 13716-24.
- . 1990. "Large Scale Purification and Immunolocalization of Bovine Uroplakins I, Ii, and Iii. Molecular Markers of Urothelial Differentiation." *J Biol Chem* 265, no. 31 (Nov 5): 19170-9.
- Wu, X. R., J. J. Medina, and T. T. Sun. 1995. "Selective Interactions of Uplia and Upib, Two Members of the Transmembrane 4 Superfamily, with Distinct Single Transmembrane-Domained Proteins in Differentiated Urothelial Cells." *J Biol Chem* 270, no. 50 (Dec 15): 29752-9.
- Yamany, T., J. Van Batavia, and C. Mendelsohn. 2014. "Formation and Regeneration of the Urothelium." *Curr Opin Organ Transplant* 19, no. 3 (Jun): 323-30. <http://dx.doi.org/10.1097/mot.0000000000000084>.
- Yang, Y., et al. 2006. "Renal Expression of Epidermal Growth Factor and Transforming Growth Factor-Beta1 in Children with Congenital Hydronephrosis." *Urology* 67, no. 4 (Apr): 817-21; discussion 821-2. <http://dx.doi.org/10.1016/j.urology.2005.10.062>.
- Yu, J., T. J. Carroll, and A. P. McMahon. 2002. "Sonic Hedgehog Regulates Proliferation and Differentiation of Mesenchymal Cells in the Mouse Metanephric Kidney." *Development* 129, no. 22 (Nov): 5301-12.
- Zhang, L., et al. 2015. "Smad2 Protects against Tgf-Beta1/Smad3-Mediated Collagen Synthesis in Human Hepatic Stellate Cells During Hepatic Fibrosis." *Mol Cell Biochem* 400, no. 1-2 (Feb): 17-28. <http://dx.doi.org/10.1007/s11010-014-2258-1>.
- Zhang, X., et al. 2001. "Cdc42 Interacts with the Exocyst and Regulates Polarized Secretion." *J Biol Chem* 276, no. 50 (Dec 14): 46745-50. <http://dx.doi.org/10.1074/jbc.M107464200>.
- Zheng, F., et al. 2002. "Upregulation of Type I Collagen by Tgf-Beta in Mesangial Cells Is Blocked by Ppargamma Activation." *Am J Physiol Renal Physiol* 282, no. 4 (Apr): F639-48. <http://dx.doi.org/10.1152/ajprenal.00189.2001>.
- Zuo, X., W. Guo, and J. H. Lipschutz. 2009. "The Exocyst Protein Sec10 Is Necessary for Primary Ciliogenesis and Cystogenesis in Vitro." *Mol Biol Cell* 20, no. 10 (May): 2522-9. <http://dx.doi.org/10.1091/mbc.E08-07-0772>.

